Universidad
Carlos III de Madrid
www.uc3m.es

Bachelor thesis on

OPTICAL IMAGING IN PRESENCE OF SCATTERING

By Pablo Bonilla Escribano

In June, 2015

Supervised by:

Tom Vettenburg

Jorge Ripoll Lorenzo

Block I: Introduction

1. MOTIVATION AND BASICS

1.1 Overview and structure of the text

This project represents a step towards the overarching aim of imaging scattering specimens. In such samples, the contrast and sharpness of optical images is severely reduced since a large fraction of the light is scattered and manifests itself as a uniform background. In optical projection tomography it has been demonstrated previously that the scattered background can be separated from the image-forming light by capturing only the first arriving photons with ingenious ultrafast gated optical set-ups [1-3]. The goal of this project is to investigate if the same can be achieved for optical microscopy using a gated camera and a low-cost laser.

In addition, this project aims to be to quantitatively stating how much the image quality can be improved using a time gated optical set-up and to enhance a 3D reconstruction of a biological tissue.

In order to accomplish the objectives, several programs and/or experiments which facilitates the everyday work in the lab were developed: like a way to orchestrate a camera, a laser, and an oscilloscope; testing two super-resolution techniques; and finding way to record data from an oscilloscope.

In short, the aforementioned set-ups are based on the same fact: if light is passed through a sample and only the first portion of the photons coming out of it are integrated to form an image, the negative effects of light scattering are reduced. To simplify the notation, I shall only refer to this idea as ‘time -gated’. This idea will be explained in detail, after the concepts of light microscopy and scattering are first introduced in this thesis.

After it, the equipment that was used in order to develop the time-gated set-up will be elucidated. These two elements makes up the introduction, the first of the five blocks onto which the text is structured. The introductory block contains all the information that was available beforehand, and after reading it, the reader should be able understand the expectations and motivations of the time-gated system before it was tested.

Then, all the experiments and programs that were performed/developed are explained in the second thematic block, followed by the third one, where the main conclusions and outlook are stated.

The rest of the blocks are self-explanatory and are included for quick reference. As can be seen, the manuscript is structured so that particular information can be found, without having to read the whole text.

It is not necessary to be an expert on imaging to completely understand the discussion, as all the needed clarifications will be included in the introduction and throughout the document.

Note that supplementary movies are included to help convey the more complex topics; the reader can watch then by clicking on the corresponding link. To make navigation more comfortable several links are included to go directly to some sections/figures within the document.

All the fonts have been automatically checked using Microsoft Word 2013 to make sure that this document is accessible and can be easily be read by people with sight disabilities. In addition, the hidden characters are optimized so that the document can be read by an automatically reading software.

1.2 Light microscopy basics

Light microscopy is a technique that uses light to obtain images of objects that fall below the eye's optical resolution. There are two main ways to do it

1) *Transmission microscopy*: where light is cast onto a **transparent enough** sample so that part of the light is absorbed by it, and other part continues its way. When a sensor is placed after the sample, *Figure 1* , it will see the 'shadow' that the sample has produced, thereby producing an image, called the projection.

Hence, a projection is actually a map of different intensities reaching the detector which are produced by the different light attenuation properties through the different paths that light follows when travelling within the sample.

A projection in itself can turn out to be very useful. In effect, the images produced by the regular light microscope are just amplified projections of samples by a lensing system.

However, studying biological tissues is a complex task, as tissues interact with other cells and with the corresponding extracellular matrix, i.e. set of proteins and other biological products that lie in-between cells, providing communication and support to them.

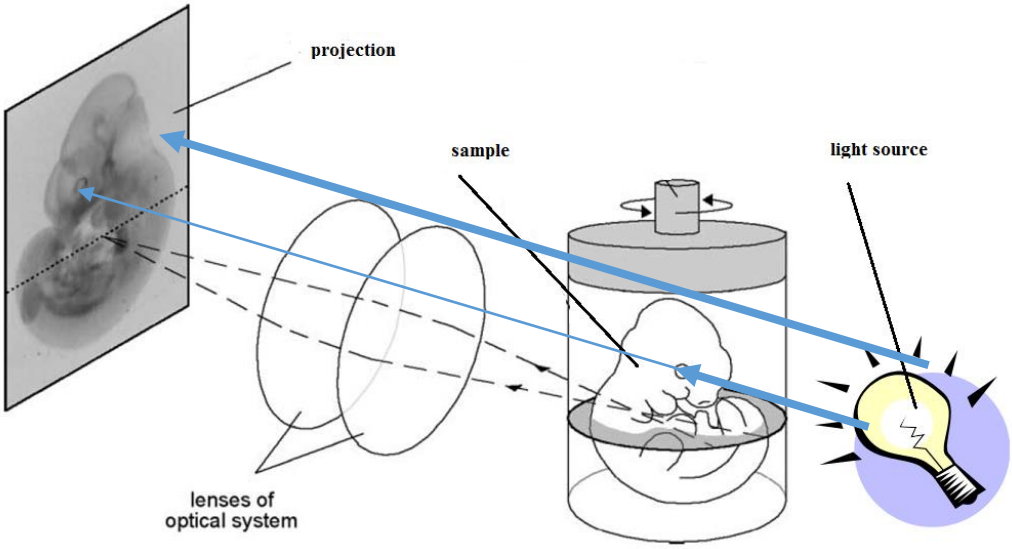

Figure 1

Example of transmission microscopy

Notice how the first light ray passes through the eye and losses its intensity, resulting in a dark area in the projection

On the other hand, the other one does not even pass through the sample, so it produces a bright area in the projection

To simply the explanation, neither the effect of the lens nor scattering is not shown (rays are depicted parallel all the time)

Source: modified from [25]

Hence, in order to understand some pathologies, it is more and more customary to reconstruct a 3D image of the sample (*Figure 2*) which in turn will allow to generate a slice of the sample without actually cutting it. This is referred to as **tomography**, from the Greek τόμος *tomos*, meaning "slice" and γράφω *graphō*, "to write".To do so, one can simply obtain the traditional projections along many angles, by rotating the detector and/or the sample, and using a reconstruction algorithm. For more details on the reconstruction methods, refer to [4].

On the other hand, there is a second kind of microscopy, what we shall refer to as **2)** *emission microscopy*, in which the light that the detector sees in not produced by an external light source, transmitted through the sample, and detected as previously stated.

In this second kind of microscopy, the light is produced *within* the sample, passes through it; and finally the light is focused with a lens system and integrated in a camera to obtain a projection of the emitted light. So a 3D rendering can also be done using the same techniques used for the other type of microscopy.

Note that in order to make the sample emit light, it can be genetically modified, for instance, making it express GFP or luciferase; the latter is the protein that makes fireflies shine during the night. In addition, the samples must also be treated with strong alcohols to make it transparent. Hence, if the sample is not inherently transparent light microscopy cannot be done *in-vivo*.

Notice that transmission microscopy is usually employed to obtain anatomical images of samples, whereas emission microscopy is more used to acquire functional images, but they are more useful if the two are registered (superimposed).

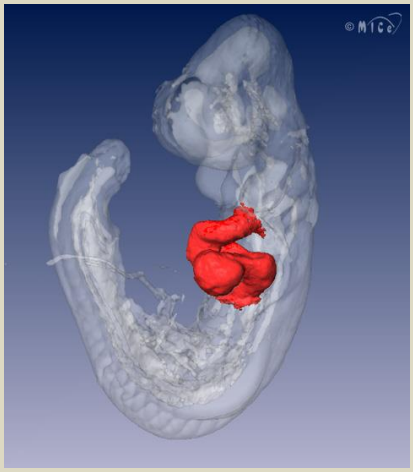

Figure 2
Example of 3D rendering
It is a E9.5 wild-type mouse embryo where the cardiac tissue is shown in red (normal development)
Source: Mouse Imaging Centre

For example, in *Figure 2* transmission microscopy was used to get the anatomical almost transparent envelope, and the cardiac cells where modified to emit light. These images were used to study the clinical significance of the TBX5 gene and to understand and try to find a cure for the Holt-Oram syndrome, which produces limb and cardiac deformations [5].

This is just an example of the many ways in which light **microscopy has greatly contributed to develop medicine**. Indeed, all the microbiology settled by Louis Pasteur and Robert Koch in the late 19th century would not have been possible without the development of light microscopy and the microscope.

In conclusion, light microscopy is an enabling technique for microbiology and medicine in general. There are two ways to implement it, however, **in both of them light is passed through a sample**, in order to produce (and possibly amplify) a projection. If several projection are taken, a 3D model of the sample can be made.

1.3 General and relevant aspects of light scattering for the discussion

It has been known since the Ancient Greeks that light *always* travels in a straight line, *Figure 3* . This is a fact [6]. However, in many of our daily life experiences it may seem that it is not always the case, *Figure 5*.

In all those situations, where an originally confined light ray widens, light continues to follow a straight line, at least at a lower scale level, for example at the nano or micro level, *Figure 4*.

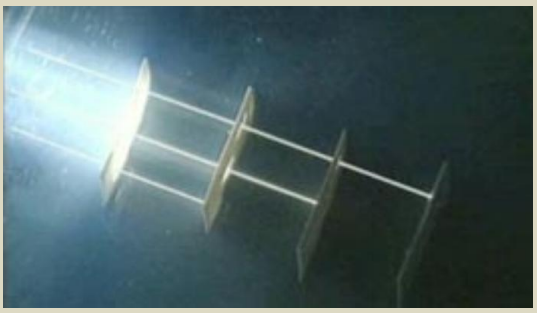

Figure 3
Simple experiment to prove that light travels in a straight path
Source: PBS LearningMedia™

As can be seen, irregularities in a medium (like a non-regular lattices), the presence of small particles, etc. deflects parts of the original parallel rays (following Snell's law) into different directions. When light reaches the end a scattering medium, there will be rays coming from many different places and orientations.

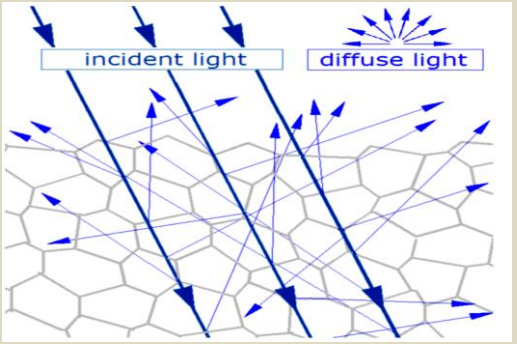

Figure 4
Schematic showing how light gets scattered
Source: Wikipedia.org

Light scattering has several implications:

1) It makes light to be loose directionality. For example, the sky is blue thanks to the fact that the Earth's atmosphere produces a kind of elastic scattering called Rayleigh/ˈreɪli/, which is more effective for short wavelengths [7]. Then, blue gets more spread and becomes more abundant than other colours such as red or green.

2) It causes attenuation of radiation in the direction of propagation. Following on the last example, near sunrise and sunset light travels a longer path through the atmosphere, as the rays impinge it more tangentially. Then, the most scattered colours, such as blue are so dispersed that are lost. On the other hand, red and orange, which have much longer wavelength are more prominent at the beginning and end of the day.

3) It makes it possible to see the white colour on objects. Strictly speaking no pigment can be white, as pigments are subtractive [8]; in other words, they create new colours when mixed with other pigments by adding their subtracting properties. For example, it is possible to get green by mixing a yellow (it absorbs every colour but red and green) and cyan (which absorbs every colour but green and blue) pigments. But in order to get white all the visible wavelengths must be added.

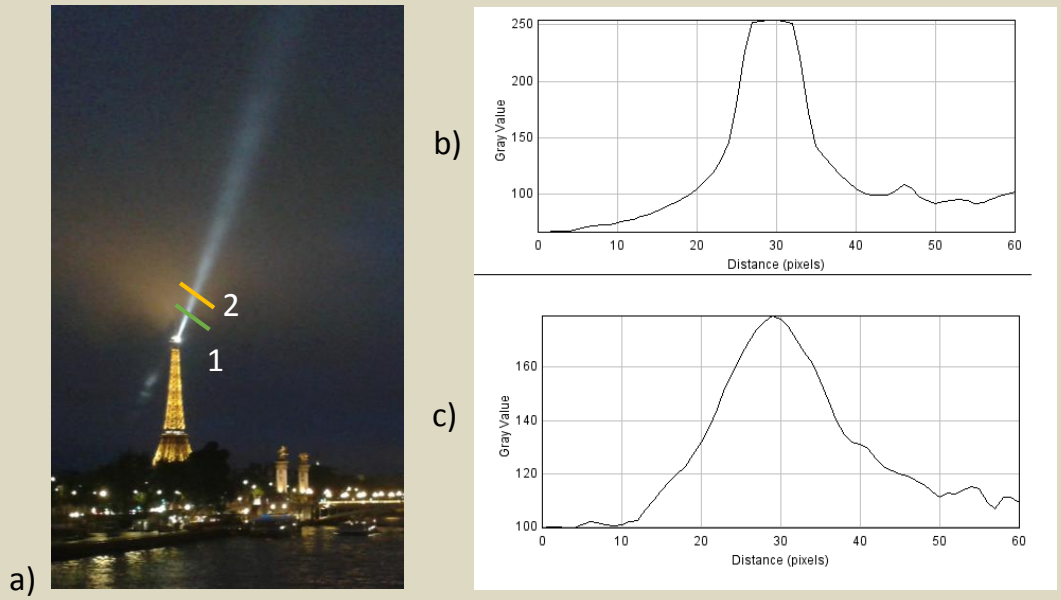

Figure 5

Simple observation showing that light does not seem to travel in a straight path

a) Original image, showing the location onto which the profiles were taken from

b) Profile along the line 1

c) Profile along the line 2

As can be seen, the width of the light beam seems to increase with distance, thus not following a straight path. It looks like the light is moving outwards and laterally form the spotlight

The scattering is produced by the drops of water that makes the fog

In effect, all the materials making up white objects, such a cotton, paper, white paint… are actually transparent! What happens is that light is so scattered when travelling through them that the different rays that compose a polychromatic light source, such as that of the Sun or a standard light bulb, are mixed in all directions in such a way they add up to yield white colour.

A very good example to understand this is a fried egg. Before frying it is transparent as the proteins (especially albumin) which are dissolved in are well-ordered. However, after it is cooked, they are *denaturized*; creating an irregular scattering medium, and gives fried eggs their white colour when illuminated with white light.

Notice, however, that this does not apply to light sources. A light source can be white, if it outputs visible light in a wide range of visible frequencies. Other important thing to remember is that white is a colour characteristic for scattering materials, but a material may also have high scattering properties and have a colour different from white.

Those all the general consequences of scattering. Now let's focus on how it affects light microscopy.

1.4 Particular and relevant aspects of scattering for light microscopy

Scattering in light microscopy has detrimental effects, and in photography in general, *Figure 6*. This is due to the first two aforementioned mentioned implications.

When the light is spread in space features are mixed, and details are lost as the image is blurred. This kind of blurring can be compared to any blurring kernel, such as the convolution with a Gaussian since the latter also mixtures adjacent pixel values. The main difference is that the 'scattering kernel' usually varies from pixel to pixel, and is difficult to predict analytically, as it is produced by an irregular medium.

Figure 6
Example of light scattering spoiling the quality of an image
The light that is scattered when travelling through the piece of scattering plastic is attenuated and spatially mixed, thereby reducing the contrast and spatial resolution
Notice how the petal creases are no longer visible
Source: Pu2Pu.com

In addition, as it has already been stated in the second implication, scattering attenuates radiation in the original direction of propagation. Notice that this attenuation is in addition to the inheriting absorption that happens when light travels through any medium. This is why many authors sum the absorption and scattering coefficients when computing the attenuation coefficient, λ [2] in the Beer-Lambert's Law, $N(x) = N_0 e^{-\int \lambda(frequency)dx}$ (See the annex for the details). The end result is that the Signal to Noise Ratio (SNR) of objects which are covered by a scattering medium decreases when doing light microscopy.

Unfortunately, **light scattering is *always* present in light microscopy**. This happens because in the two kinds of microscopy (either transmission or emission) light must always pass through the biological sample in order to make a projection, but biological samples usually have high scattering properties [9].

There are mainly two reasons to explain it:

1) Cells are living units that have several specialized compartments to perform particular tasks, i.e. organelles. Indeed, the fate that a light ray will have if it crosses a cell by the Golgi apparatus has nothing to do if it crosses a mitochondrion. In addition, if a whole tissue is under study, light will see harsh and irregular transitions between the different layers, e.g. from tunica intima, media and adventitia when passing through a vein or artery. This makes light be reflected into very different directions, thereby scattering it.

2) Some cells store highly scattering substances, for example, adiposities store fat in the form of drops.

Even when the samples are made transparent, some reaming scattering stays in the sample and /or the medium.

In fact, light is so scattered when travelling through some tissues that some authors have tried to fit the propagation of light through tissues using the diffusion equation, in order to increase the resolution [10].

1.5 The time-gated set-up as a way to avoid scattering

At this point, the reader should be able to be fully aware of what is scattering and why there is a *real* need to get rid of it in imaging, and thus to understand the aim of this thesis.

Only in three publications this idea has been implemented ([1] [2] [3]), so far. The time-gated set-up consist of using a camera so fast and with a gain so powerful that it can make a projection before the scattered photons arrive to the detector. Notice that this makes sense as the speed of light is constant inside a medium, i.e. both scattered and forward moving photons travel at the same speed. Hence, if the medium is not extremely scattering (in the sense that some photons are not scattered) scattered photons will arrive later in time as they have to travel more distance.

To understand this better, watch the Complementary movie 1. This represents a slice of a rectangular sample being imaged (green). Both the sample and the medium makes light to be scattered (at the red dots). The image that is shown in the sensor was simulated by increasing discs of Gaussian blurring of a black rectangle on a white background. The image represent the acquisition that is obtained by integrating all the photons that have arrived until that instant. Notice that each time, all the photons move the one arrow length.

In order for this idea to be possible, a pulsed source of light is needed. For example, if a Continuous Wave (CW) or a light source producing long light pulses (in time) is used, when it will be impossible to discriminate between the scattered and non-scattered photons.

1.6 Implementation of the time-gated set-up in this project (SPIM)

So far, this idea has been implemented in transmission microscopy, using the set-up shown in *Figure 1*, which is called OPT. However, the 'sample' has been either a phantom or the 1951 U.S. Air Force target (a target that contains series of lines patterns with increasing spatial frequency, used to know the resolution of an imaging system).

Hence, this project aims to image a biological tissue using the time-gated idea by means of a different microscopy set-up. Out of all the different light microscopy techniques that there are available to do it, SPIM was selected. The reader should see why after reading how it is put into practice. A SPIM implementation is shown in *Figure 7*.

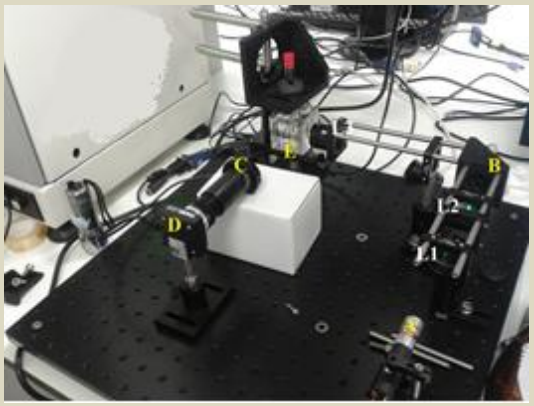

Figure 7
Implementation of *SPIM*
A) Laser
B) Mirror
C) Lens to focus on the plane
E) Sample on moving platform
L1 and L2 are two lenses used to span the laser beam. L3 is a cylindrical lends.
Notice that the increase in size of the beam can be seen in the picture

The idea is that the laser beam (produced in A) is widened by the two lens (L1 and L2). Then, the light beam is reflected into a mirror to save space (B). And it is finally cast onto a cylindrical lens that will convert it into a light sheet that will illuminate the sample.

Such light sheet ranges from a few micrometres. This fact explains why SPIM produces low photo-bleaching and makes it possible to image for long periods of time: only the thin section that is imaged is illuminated. In addition, the good sectioning capabilities decrease the background signal, thus yielding a higher contrast, which is even compared to that of the Confocal Microscopy.

Next, the camera (D) will take an image of the sample perpendicular to the illumination direction. A lens (C) is used to focus the image.

Once the image is taken, the sample (which is attached to a moving platform, (E) is laterally shifted. This process is repeated until the whole sample is imaged, in such a way that a 3D reconstruction is possible by taking enough projections.

Note that it is necessarily to widen the light beam coming from the laser before it reaches the cylindrical lens, as otherwise the sample would be illuminated with a light pattern closer to a line rather than a sheet of light.

Based on the fact that the parallel rays to the principal axis fall on the focal point of convex lenses [11] it is possible to expand the beam coming from the laser as shown in *Figure 8*.

As the angles are equal,

$$\tan\alpha = \frac{H_1}{F_1} = \tan\alpha = \frac{H_2}{F_2}$$

So, if F_1 and F_2 are the focal distances of the lenses,

$$\frac{H_2}{H_1} = \frac{F_2}{F_1}$$

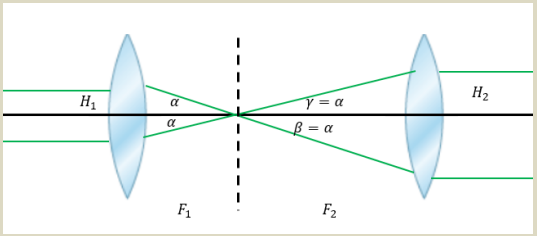

Figure 8

Widening a beam

Notice that when one focal point is shared between the two converging lens, β=α because they are angles opposed by the vertex; γ=α by symmetry, and the remaining angle must also be α, as it is equal to γ. So the four angles are equal. The principal axis is the black horizontal solid line in this case

2. MATERIALS AND METHODS

2.1 Camera

The selected camera for the time-gated implementation was the ICC DH334T-18U-03 (iStar). Where the '18' means that the camera has an 18mm image intensifier diameter, the 'U' stands for ultra-fast gating speed (~2ns), and the '03' refers to the image intensifier material: W-AGT photocathode, P43 phosphor (not relevant for our discussion). It also has a fill factor of 100% and a pixel size of 13.3μm, but a FWHM of 26.1μm (reported by the manufacturer for a single photoelectron event at high gain).

This camera is actually optimized for making fast spectrometric measurements [12] at low light levels, as can be seen in the number of spectrographs which are compatible with it and how the manual put an emphasis on the different options it has to improve spectrographic measurements, like the different image intensifying materials.

For this project, the camera have three relevant features:

1) It is gated. That is, it can be turned on and off very fast. To achieve it, the camera does not employ mechanical shutters, since they are unreliable and for practical reasons they are limited to a few Herts (Hz). Hence, it has a photocathode, i.e. a material that produces free electrons when light strikes it. When light is converted into electrons, they can only move if they are subjected to an electric field. Thus, the camera allows light to pass by controlling the electric field on the photocathode. If the electrons are allowed to pass, they will impinge a phosphor (a material that produces light when electrons hit it), thereby tuning then into light again.

2) It has high gain. When short integration time are used, the SNR decreases proportionately as the number of photons reaching the detector decreases and the shot noise increases. To solve for it, the camera has two ways increase the gain.

First of all, it can increase the number of electrons which are in the silicon chip prior to readout, as any regular CCD camera. The term '**regular gain**' will be used to refer to the gain of the camera when this kind of gain is unity, regardless of the value of the next other type of gain.

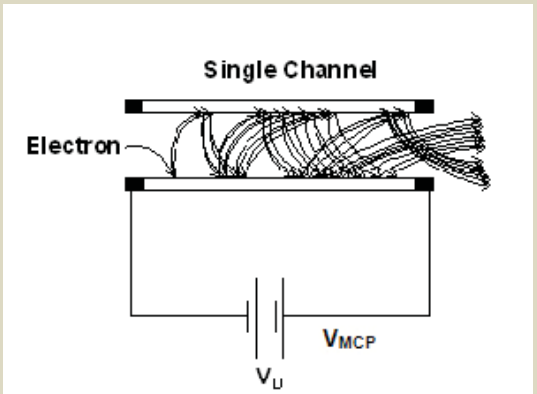

Figure 9
Micro Channel Plate
Notice that the voltage of the MCP (V_{MCP}) that is used to increase the number of electrons via secondary emissions is independent from that is used to allow them to them reach the MCP
Source: iStar's user's manual

Secondly, it has a Micro Channel Plate (MCP), which is a thin disk of 'honeycomb' glass, which is coated with a resistive material. It has a high electric potential across it, from 500V to 1 000V so that electrons cascade drown, thanks to the secondary emission of electrons, *Figure 9*. Its name roots from the fact that each individual channel is ~10 μm wide.

3) It has several Digital Delay Generators (DDG's). They are electrical circuits that produces an electrical signal after a trigger input is produced. They are necessary to synchronize the acquisition with the output in of the light source for certain types of set-up. Usually, they have to be bought separately and connected to the instruments, like in [1], but it is very handy that the camera have them already embedded.

2.2 Electrical signals of the camera

The camera has several electrical outputs which, when seen in an oscilloscope, reveal useful information about what the camera is doing. Many screenshots from an oscilloscope will be shown in some figures throughout the document, so the meaning of the signals is explained in detail in *Figure 10*. Most of the electrical connections are accessible from the back of the camera, and have a SMA connection. The only exception is the gate pulse, which is located in one lateral and needs an especial connector which is supplied with the camera, *Figure 11*.

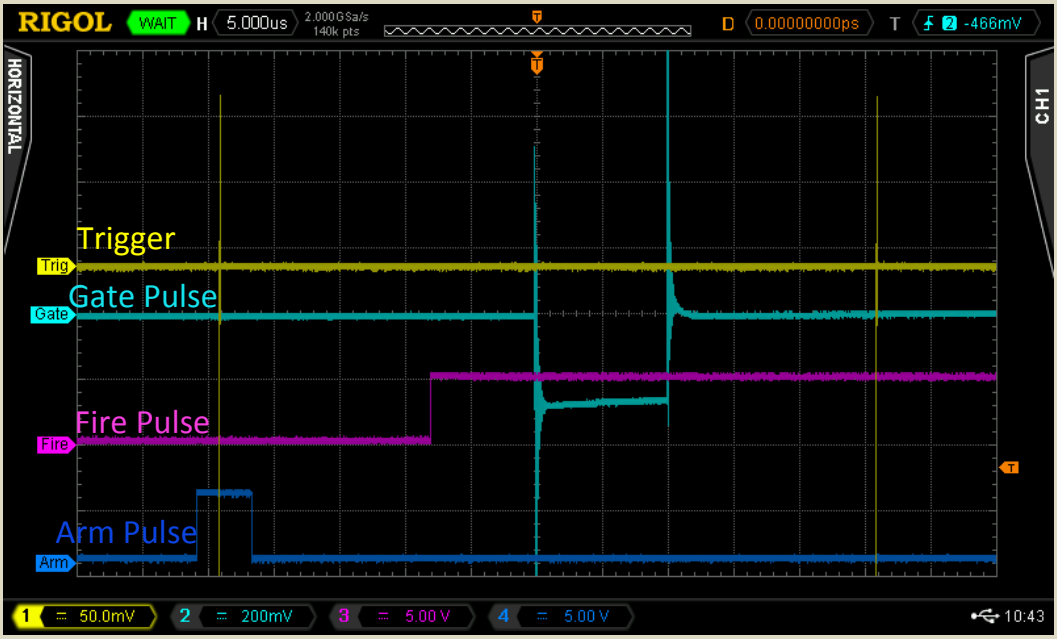

Figure 10

Electrical pulses from the camera

Channel 1 (Trig): Electrical signal from the laser indicating that a light pulse has been sent, one per peak. Notice that the trigger signal shown follows the NIM standard, but the camera only accepts TLL signals.

Channel 2 (Gate): Gate pulse. The camera allows electrons to reach MCP in the time between the low and high peaks. If the MCP is also gated, an extra small peak appears first, indicating that the MCP is on, like in *Figure 14*

Channel 3 (Fire): Fire pulse. It is HIGH (5V) when the camera is in the accumulation period. In other words, all the light that is allow to pass then this signal is HIGH (5V) will be integrated on the CCD chip to produce one single image. It is LOW (0V) when the camera is reading an acquisition; or it is doing a series of row and columns shift on the chip, in order to remove any remaining electron on the CCD, before a new acquisition is taken; or else when the CCD is not on.

Channel 4 (Arm): Arm pulse. It is HIGH (5V) when it is ready to be triggered by the electrical signal from the laser, and it goes LOW (0V) when it will ignore the external triggers (as it is acquiring, processing an image or removing any remaining electrons on the CCD chip)

The optimal trigger settings are selecting the rising edge of the gate pulse at around half of the lower peak

2.3 Light sources

In this case, a monochromatic light source is needed, because light is scattered and absorbed differently depending on the frequency of the light, as explained by Snell and Beer-Lambert's laws. Otherwise, it will be very difficult to find the optimum gating time, as each wavelength would have its own time window in which non-scattered photons are arriving.

At the time of writing there were only two pulsed lasers at my disposal which produce an electrical signal each time they send a laser beam:

1) The MPL-N-532 which outputs a laser beam at 532±1nm with an **unpredictable** repetition rate [13], from 5 to 15 kHz. This is because it is meant to be used in industry for marking on highly reflective metals, ceramics and composites, so even scattered light from it can produce skin burns. This also explains its high power. It also has long pulse duration (~5ns). When it sends a light pulse it produces a TTL signal.

2) The EPL-670 which allows the user to select several repetition rates and which produces a light at 669-675nm. This laser has much lower power than the previous one (the max peak power @10MHz is just 75mW [14]), and the pulse width is also much sorter (less than 100ps). When it sends a light pulse it produces a NIM signal.

Hereafter, they will be referred to as green and red lasers, respectively.

Note that the aforementioned lasers cannot be triggered by an external device, **under normal operation**.

Block II: Experiments

1. PREPARING THE CAMERA

1.1 Protecting the camera

As the camera is going to be used at very high gains, even the light used to illuminate the lab would more than enough to trigger an electron flow so strong inside the MCP that the camera would be permanently broken. In addition, the quantum efficiency of the photocathode is greatly compromised if photo-bleaching occurs even if the camera is turned off. These kinds of damages are not covered by the warranty [15].

Thus, a light proof structure was built, *Figure 11*. This consist of a rigid scaffolding that was attached to the table using compatible posts and post holders and a ma-

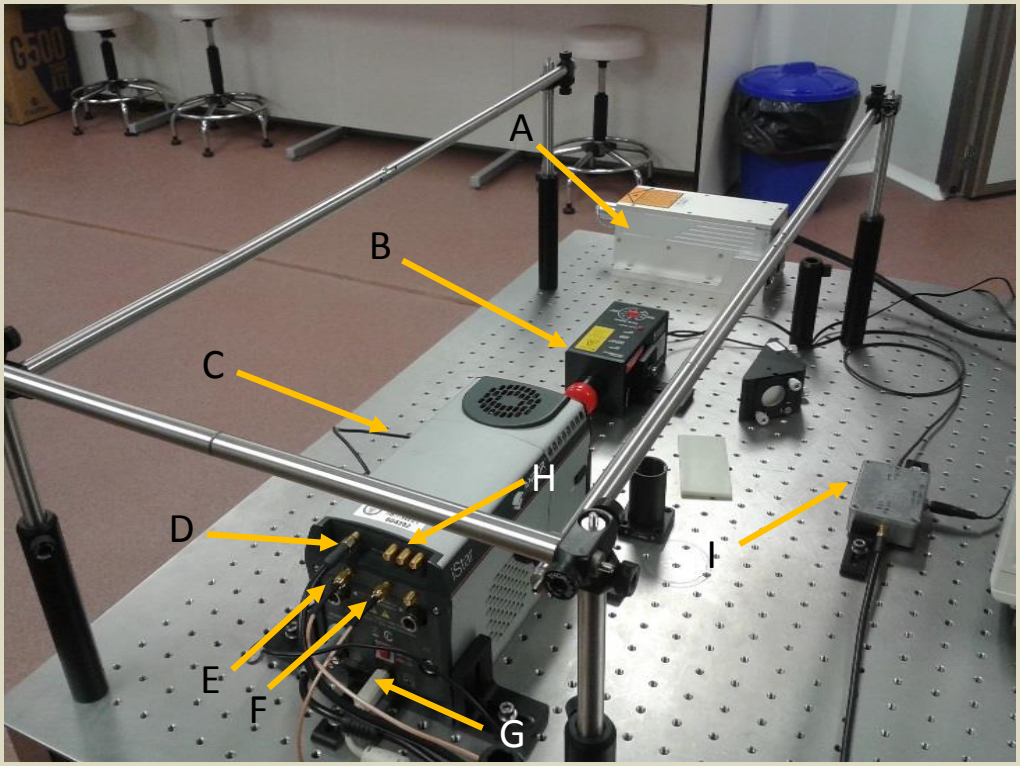

Figure 11

Building the light proof structure

A) Green laser
B) Red laser
C) Gate pulse connector (especial connector)
D) External trigger connector (SMA)
E) Fire pulse connector (SMA)
F) Arm pulse connector (SMA)
G) USB connector, since the camera is controlled by a computer software
H) 3 outputs (SMA)
I) TTL converter, which will be explained latter

-terial to cover it. Notice, however, that there were not enough posts to make the scaffolding, so the missing ones were substituted by posts made of folded paper.

There are three ideal features for the material to close the structure:

1) It must have high light absorbance properties. Not only this is important to prevent the external light from reaching the camera, not also to avoid reflections from the laser that may cast light onto the camera's case and/or the operator. Recall that a powerful, and thus dangerous laser was to be used.

2) For the same reason, it must be have good fire resistant properties.

3) I must have a reasonable price.

The chosen material to close the structure was thick black cardboard and electric tape to cover the boundaries. In fact, the black cardboard was more efficient preventing light from going through it than a specialized blackout fabric. Notice that it was thick in order to make it relatively fire resistant.

Other considered material was aluminium, due to the fact that it has a heat conductivity is 2 to 4 times greater than that of the steel [16], making it a relatively good, cheap, and fire resistant material, but it was rejected due to its reflecting properties.

In the process of looking of light absolving materials, it was found that some jeans are more light absorbent than many black tissues, as the latter are usually arranged in patterns where the threads are quite far away to be elastic.

To make sure that the protection was enough, the following protocol was followed: The lights in the lab were turned off, and the camera was set to half the maximum regular gain to make 2s acquisition in a continuous way at -5°. In order to maximize the number of possible photons reaching the camera from all possible directions, no lens was attached to it. Then, the light proof structure was illuminated with the white, diffuse and LED light (at the maximum intensity) of the GT-I8190 mobile phone to try to see if the camera can see the light going through it;

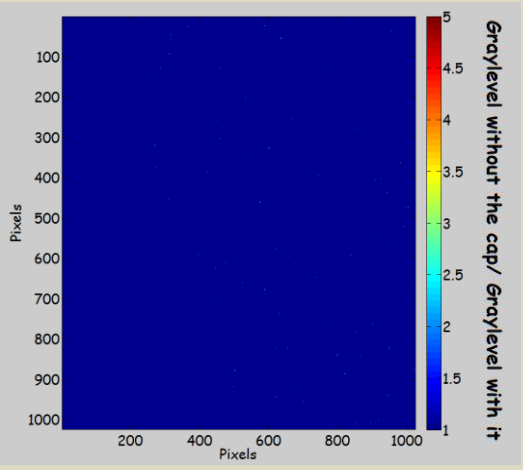

Figure 12

Quantifying the light proof cage

Notice the small values of the colour-map

The conclusion is that the camera can be used with the lights being on, so that more people can work simultaneously in the lab

and if that was the case, the problem was corrected. This process was repeated until no light was visible.

Finally, once the light proof cage was safe enough, it was quantified by taking a 5s acquisition at maximum regular gain with the lab's lights on and without any lensing system, and dividing it by other image taken with the cap of the camera closing its aperture (i.e. ideally an image of dark current of the camera), *Figure 12*.

1.2 Limitations of the camera

Once it was save to use the camera, the author performed a series of experiments to see its limitations, thereby advoiding future unexpected behaviours.

It was found that the **actual length of the fire pulse**, as measured in an oscilloscope, and the one **set by the software of the camera were different for values strictly smaller than 80μs**. When the user selects a value below 80μs the measured length will always be 70.4μs; even if the set value is as low as 10μs, which corresponds with the minimum selectable fire pulse length.

In addition, it was discovered that the **fire pulse**, under some circumstances, becomes **unreliable**, in the sense that it is so delayed that the gate pulse precedes it, *Figure 13*. A careful reader would understand that this does not have any sense: if that were true, then the camera would be allowing light to reach the CDD when the chip is not integrating the light that reaches it.

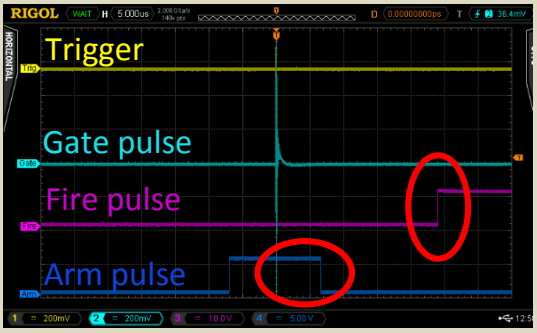

Figure 13
Defects of the electrical signals
Notice that the external trigger cannot be seen because it is under the gate pulse
Channel 1 (Trig): trigger pulse
Channel 2 (Gate): gate pulse
Channel 3 (Fire): fire pulse
Channel 4 (Arm): Arm pulse

After contacting the camera's supplier, who, in turn, forward the question to the manufacturer, we reach to the conclusion that the camera is working correctly, the only problem is that the fire pulse is delayed.

This happens because the Fire pulse does not go HIGH (5V) after the camera has performed a series of row and column shifts in the CCD chip to clean any remaining electrons after the previous acquisition. A solution would be to use the **outputs A/B/C as a reliable CCD reference.**

Other limitation was the fact that the arm pulse takes up to 8 μs to reach 0V instead of going immediately to 0V when it receives an external trigger, *Figure 13*.

With regard the gate pulse, it is the most stable one. However, the voltage of its peaks changes with the selected time width. Hence, sometimes, the voltage scale was changed to accommodate for these differences. Other problem, was that it was very difficult to see at which instant the two peaks appear for values lower than 150ns, because they are not actually two clean peaks, as they decrease to 0 as an exponentially decreasing sinusoidal function, i.e. underdamped response, *Figure 14*.

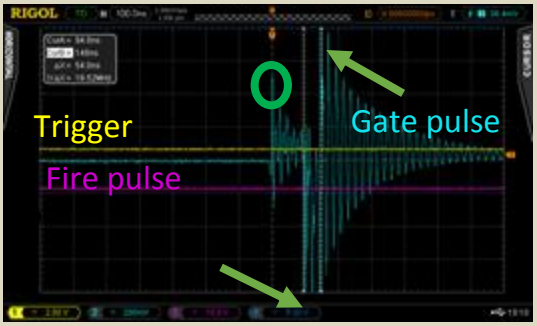

Figure 14

Detail of the gate pulse

When the light is allowed to reach the CCD for times smaller than 150ns, it is difficult to see the two peaks (at the arrows).

The encircled peak represents the MCP being gated, i.e. turned on

Compare this image with *Figure 10*

The camera can be controlled by a computer application, called *Solis for Time-Resolved*, which can run programs written in *AndorBasic*. However, most of *AndorBasic* commands are outdated and cannot be used with the camera. In addition, the needed software development kit is not free. So the only practical way to control the camera is using the user interface of the *Solis for Time-Resolved* software.

It was also discovered that when the camera is set the maximum possible gain (also increasing the gain of the CCD chip) and it is set to only record the pixels

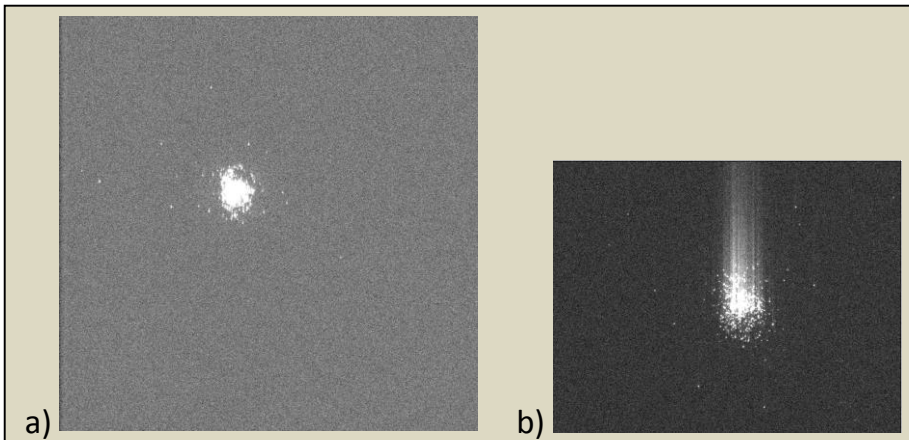

Figure 15

Smearing of the images at the maximum possible gain

a) Image obtained at full resolution, 1024x1024 pixels

b) Image obtained selecting a region near the laser same light pulse, 518x403 pixels

Note that the background looks different as the contrast was enhanced for the two images separately. Mote that the maximum grey level was 2 373, so the artefact is not caused by saturation

values of one portion, the image is smeared in the vertical direction, *Figure 15*. This kind of 'smearing' is technically known as 'bleeding' for image sensors.

However, it was checked that the gain of each pixel was homogenous when the camera was illuminated with the white, diffuse LED light (set at low intensity) of the GT-I8190 mobile phone, so no corrections in the gain were to be applied.

1.3 Focusing the camera

In order to clearly see any feature with a camera, it must be focused. In this project, this was achieved by a single 60mm lens, which was attached to the camera's aperture by an adaptor and some lens tubes. The lens have short focal length in order to reduce the required spaced inside the light cage, by bringing the focal point closer.

When focusing the camera, one should have an estimate of the details which can be seen when the camera is focused, in order to be sure that the camera is as focused as possible. In the absence of optical aberrations, the Airy disc, that is, the light pattern which is produced when light produces an interferometry pattern when passing through a circular aperture, is an upper bound for the resolution of the system.

The Airy disc is computed taking into account the fraction of light which is allowed to reach the detector. In this case, 50mm of lens tube were placed between the camera and the lens. In addition, 150mm of lends tube were also added between the lens and an iris of 5mm diameter at the opposite end of the camera, to prevent light coming from reflections. Hence, the Numerical Aperture (NA) will be given by:

$$NA = \frac{2.5}{\sqrt{(150+50)^2 + (2.5)^2}} = 0.012$$

Hence, the smaller visible detail would be seen for the longest used wavelength: $Resolution\ [17] = 0.61\frac{\lambda}{NA} = 0.61 \times \frac{675nm}{0.012} \cong 41\mu m.$

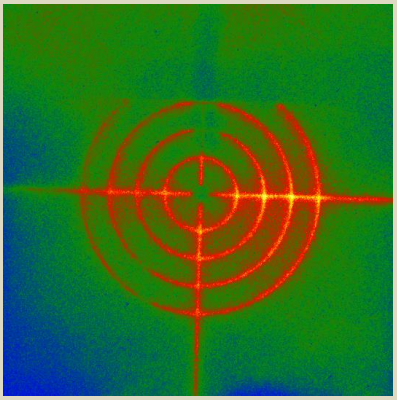

Figure 16

Using the target to focus

The target is a piece of metal which has a pinhole of 1 mm and the shown pattern, *Figure 21* Notice that the illumination is inhomogeneous This process was speed up using the lens equation $\frac{1}{f} = \frac{1}{a} + \frac{1}{b}$, where f is the focal distance and a and b are the distances to the lens. Once f=60mm and a=50mm were fixed, then b≅ 150mm

Note that there is demagnification of 2, so that the signal each pixel receives is increased. Then, the light proof cage is opened from the opposite end of the camera, so that the pattern in a target is illuminated. Then the camera is moved until small details, of around $41\mu m$ are visible, *Figure 16*. Note that this *estimation* is correct since the white light used to illuminate the lab also contains red light.

Finally the camera is fixed and the position of the target is flagged. If a **liquid sample is used, then this procedure must be done with water in the sample container**, because the difference in the index of refraction between air and the liquid may change the focal point in the order of ~5cm.

1.4 Temperature and avoiding stress

This ICCD camera has a thermoelectric cooling that is used to cool the electronics down to -25° in around 15 minutes, thereby reducing the dark current and improving the SNR. This this also controlled by software. However, over the course of the first experiments, it was determined that a temperature as high as -5° was more than enough. In particular, the noise levels were 743 for -5°, 692 for -10° and 646 for -25°.They are the mean of a rectangle of 1223 $pixels^2$, measured in grey levels of a 16-bit digital signal, i.e. the maximum is $2^{16} - 1 = 65535$. They were obtained integrating at maximum regular gain with the cap closing the camera for 2s.

This small difference in the noise level was not essential for the experiments, so most of the time, the -5° temperature point was set, unless the lab's air conditioning was on. This was very important, as it was not possible to follow the safety & and warnings' directive of the camera that states that the camera needs at least 100mm of clearance distance in front of all the ventilation slots, due to the lack of space.

Nevertheless, in order to prevent overheating, the following protocol was always followed after each acquisition was completed: 1) the MCP gain was set to 0, i.e. the minimum value 2) the laser was turned off 3) the top part of the light proof cage were removed, allowing the user to change sample and to let the camera 'breathe' for at least 1 minute.

Another possible solution would have been to have used a water chilling system, as the camera includes the connectors, but it wasn't available in the lab.

2. DIFFERENT WAYS TO IMPLEMENT THE TIME-GATED SYSTEM

2.1 Thinking on the different possibilities

As can be seen, understanding and properly controlling the camera was one of the very first aims, and by itself it took quite a long time. Once the camera was

ready to be used, the author was ready to use it for the general propose of the thesis: **reduce the presence scattering of the light microscopy images by only looking at the first-arriving, less scattered photons**.

Of course, the **first question that must be answered, even before implementing the SPIM** (or in general to any light microscopy system) is *when* the first arriving photons will reach the detector. In other words, what would be the optimal gating time?

To do so, the light pulses should be analysed and reconstructed in time. For that, a short light pulse must be made to pass through a scattering material, and several images must be made with known time delays should be made in order to see at which time delay most of the photons were not scattered.

Hence some form of synchronization, either when obtaining the measurements or after it, is needed between the camera and the pulsed light source, in other to know when an image was taken with respect to the time that the laser started sending the light pulse.

Only considering the two available lasers, there are mainly three approaches to synchronize the camera with them, namely: taking images at fixed rate, delaying the laser's light pulses; and imaging at next light pulse. They are explained in detail in the next sections.

2.2 Imaging at next light pulse

This consist of setting the camera to take an image with a delay from one trigger electrical pulse so long that the camera integrates a part of the next light pulse,

Figure 17.

This implies that the firing rate of the pulse must be predictable, and, in fact, the error the laser has when sending the pulses in a regular fashion would be an upper bound in the time resolution of the final reconstructed profile. This is a streamlined approach that takes advantage of the camera potential, even if only one image is recorded every two light pulses.

Notice that the elapsed time between the trigger pulses and the beginning of the light pulse must be constant enough for this idea to work.

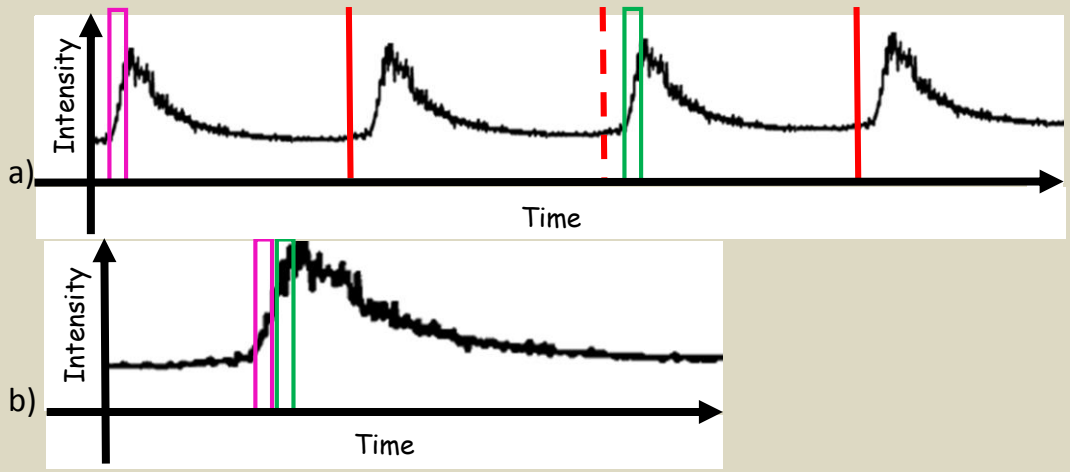

Figure 17

Imaging at the next light pulse

a) Light intensity reaching the camera after passing through a scattering material. Time goes from left to right. Each rectangle represent the portion that is integrated by the camera. The solid red lines represent the trigger signal sent by the laser used to set the reference time point to add a delay which will be increased each time. The dashed red lines are the triggers which are ignored by the camera. In this case, the laser must has a regular firing rate, so that each time it is possible to know which part of the next pulse has been scanned

b) Reconstruction after sorting all the recorded acquisitions. Note that the only information that was reconstructed is the one that is inside the rectangles. In order to completely reconstruct the pulse, more samples must be taken. Overlapping may occur.

Source: The single energy pulse was taken from [2]

2.3 Delaying the laser's light pulses

In this scheme, the laser beam is made to pass through an optical fibre, it is reflected into seral mirrors, or else the laser is placed far away from the camera, so that by the time it reaches the ICCD camera, it is ready to image the pulse. The time evolution of the pulse is obtained by changing the relative delay between the trigger pulse and the opening of the photocathode.

The main advantage, is that the pulsed laser does not have to have a repeatable firing rate at all, provided the time distance between the trigger pulse and the time it starts casting the laser is stable enough.

2.4 Taking images at a fixed rate

This is the simplest synchronization set-up, as the synchronization is be performed *after* the images are taken. Therefore, the camera is programmed to take images with short integration time, i.e. the distance between the two peaks of

the gate pulse is small, in order to have a reasonable time resolution to determine the optimum gate time.

Of course, when doing so, the camera would be taking many images, and each one of them would belong to a different time instants of the different pulses that are sent by the laser,

Figure 18.

But, how to programmatically and easily know when each image was acquired so that it can be sorted? Using information from the trigger of the laser. To do that, an oscilloscope cold be used to record the gate pulse each time an image is taken.

This method has the advantage that the firing rate of the laser does not have to be predictable. The only requirement is that the time between the electrical signal of the laser and the instant it casts light is regular for all pulses.

When sorting the data, overlapping may occur. When this happens the corresponding acquisitions may be averaged, yielding a high SNR profile of one single pulse.

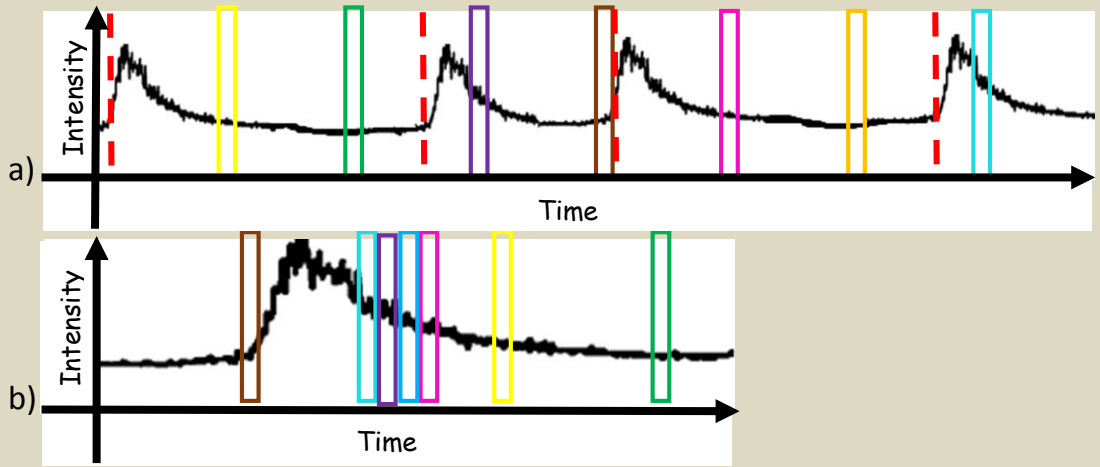

Figure 18

Taking images at a fixed rate

a) Light intensity reaching the camera after passing through a scattering material. Time goes from left to right. Each rectangle represent the portion that is integrated by the camera. The dashed red line represents the trigger signal sent by the laser, which are ignored. This idea can also be implemented for laser with regular firing rate. But for them, other idea is much more efficient

b) Reconstruction after sorting all the recorded acquisitions. Note that the only information that was reconstructed is the one that is inside the rectangles. In order to completely reconstruct the pulse, more samples must be taken. Overlapping may occur.

Source: The single energy pulse was taken from [2]

However, this way of doing it has several drawbacks: first of all, it squanders all the synchronization capabilities of the camera. Secondly, it is likely to produce several Megabytes of data which can only be used to shape one single pulse. Thirdly, most of the most of the images (and thus time) will be useless because it misses the pulse.

For instance, if one tries to catch a 5ns light pulse that appears every 50 μs by taking acquisitions completely at random but not repeating any value, and opening the photocathode for 5ns, the probability of finding it would be 1:10 000. However, for comparison, the probability of correctly choosing 4 regular balls and the bonus one in the UK's National lottery is *higher* [18].

Other limitation is that the time between the trigger and light pulses must be constant for this idea to work.

3. IMPLEMENTATION OF 'IMAGING AT THE NEXT PULSE'

3.1 Characterization of the trigger pulses

The first step that must be done when developing this idea is to find a way to quantize how predictable the trigger of the lasers are, in order to give a precise upper bound for the time resolution. To do so, the trigger signal was recorded using an oscilloscope, for around one minute and a half.

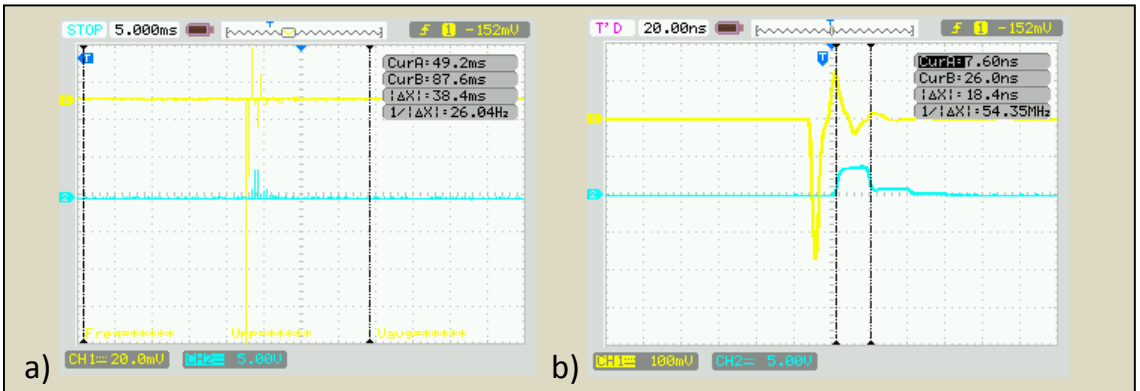

Figure 19

Looking at peaks that have low repetition frequency

a) Image obtained with the normal mode

b) Image obtained with the 'Peak detect' mode. In this mode, the oscilloscope stores the maximum and minimum value of many recordings, over the sample interval that otherwise would have been shown on the screen. Then it uses that information to get the envelope of the signal to recover the narrow pulse that was lost. No additional details are included in the manual [24]

There are several nuances that must be taken into account: first of all, to clearly see the pulses, the 'Peak detection' mode may need to be selected. This happens because some oscilloscopes, like the DS1104B, reduce their sample frequency when looking at big time intervals, in such a way that short pulses are lost, *Figure 19*. Then, a program written in LabVIEW (see it in the annex) was used to obtain

'screenshots' of the oscilloscope's screen to save them in a file. In order to know the sample rate, and thus be able to determine the time error of the trigger pulses, the program asks the oscilloscope for the sample rate, and appends it to the name of the file.

Before contacting the oscilloscope's technical support, this was done by retrieving the time base, that is, the time distance in each of the big divisions of the oscilloscope screen, and then using this relationship: $Sample\ rate = \frac{\text{number of pixels on the screen}}{\text{screen}} \cdot \frac{\text{screen}}{\text{number of divisions on the screen}} \cdot 1\frac{\text{division}}{\text{time base}} \cdot 1\frac{\text{pixel}}{\text{sample}}$. However, even if this idea also works, not only is this procedure more difficult, but also less generalizable, as the number of pixels and divisions on the oscilloscope's screen changes from oscilloscope to oscilloscope. This was important in this project, because of the fact that up to three different oscilloscope models were used, depending on their availability each day.

Other thing that was clarified thanks to the technical support were the strange peaks that appeared between each screenshot,

Figure 20.These are actually a header which consist on a header denoter, '#'; followed by N, which is a number that means that there are N bytes following it which will tell the length of the data points sent by the oscilloscope in ASCII characters. Finally, a terminator is placed at the end of the communication.

With this information, and the fact that N is always equal to 9 [19], the headers were removed when reading the data files. Indeed, it could have been directly removed in the LabVIEW program, but it was decided that it was a good idea to keep them, in order to have a clear reference to separate the different screenshot when processing the data.With regard to the file type, the data was first saved in ASCII format, but the time to process one single file was of the order of minutes. The execution time could not be significantly reduced by saving each acquisition into smaller files.

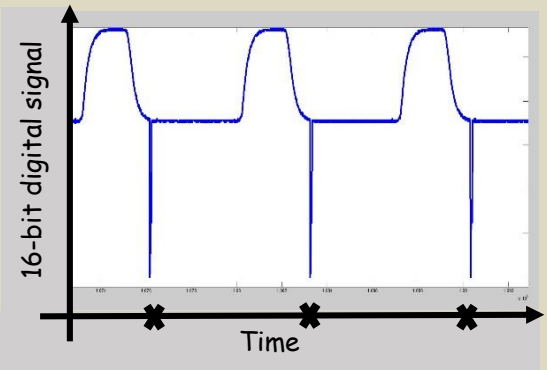

Figure 20

Raw data from the oscilloscope

The x axis is time. Its units are not shown, because it is discontinuous each time the oscilloscope sends data from different screenshots, which can clearly be seen by the peaks (and it is indicated by the crosses in the axis).

The y axis is the magnitude of the 16-bit signal, which was not converted into the voltage value, as it was not needed

The effective solution was, then, to save the data in a binary file. The computational time was reduced by a factor of 15.

To process the data, a different program written in the Matlab language was used (see a link in the annex to download it with some representative data).

Two ways to estimate the time error were implemented on it:

1) Using the standard deviation of the time distance from the beginning of each screenshot to a reference point. Such a reference point is was calculated using linear interpolation to find the first sample whose digitized signal was greater than a threshold. The threshold value was calculated as the mean of the median of the 10 smaller and 10 greatest y values of the first acquisition, if the pulse is positive; and if the pulse is negative, the best threshold found was double the minimum value.

2) And other one, which employs a super-resolution technique [20]. This is algorithm is designed for looking for the correlation of two input functions, $f(x,y)$ and $g(x,y)$, which are offset by an amount $\vec{u}$. Then, it finds the $\vec{u}$ that minimizes the integral of the squared difference between $f(x,y)$ and $g[(x,y) - \vec{u}]$, that is $\left|\left|f(x,y) \times g[(x,y) - \vec{u}]\right|\right|^2$. This is done using the **correlation theorem**, which states that multiplying the FFT of one function by the complex conjugate of the FFT of the other gives the FFT of their correlation. If the previous step is performed by multiplying the FFT of two zero-padded data from two oscilloscope's data by a factor N, then the offset $\vec{u}$ (and thus a good estimate of the time error of the repeatability of the laser) can be determined with an accuracy of $\frac{originalresolution}{N}$.

The used algorithm does this efficiently by only computing the FFT around the minimum obtained with a padding factor of 2, since zero-padding can bias the result and is memory demanding. Note that this idea directly works for 1D signals, even if it was originally developed for 2D.

After all this discussion, it was shown that the time error of the **red laser was below 0.1 ns for all its firing rate configurations**. However the **green laser** was clearly **unpredictable**, just looking at the oscilloscope so it cannot be used to develop this idea.

3.2 Obtaining images to know the optimal gating time

Once it was decided that the red laser was the only suitable one to be used when imaging at the next light pulse, its light beam was expanded to double its diameter with two lens of 50 and 100mm (as it was explained in the introduction).

After focusing the camera as it has been described, the light pulse was made to pass through a pinhole of known size, 1mm, and then through the scattering sample, so that scattered light gets delayed by a measurable amount, and the optimal time delay to take images can be obtained, *Figure 21*.

With regard the scattering sample, as a first attempt, a phantom made of plastic, with some holes inside it, was used. However, it was too absorbent/scattering for the weak light from the red laser to through it, so it was discarded.

Notice that a sample with some holes or with a sharp edge is very useful, because it can be used to more easily see features becoming 'coarser' when the scattered photons arrive. Other ideal characteristic is that it has white colour, since, as said in the introduction, white colour is characteristic of high light scattering. Other good characteristic is that the sample is be liquid, so that many dilutions with known properties can be explored.

Therefore, combinations of full milk (3.6g of fat per 100mL) with water were made and tested in a small plastic cuvette. However, the small cuvette was not long enough to allow the scattered photons to be significantly delayed, so that more than two frames are obtained from one single light pulse, even when the camera is working at the minimum gating speed, i.e. 2ns.

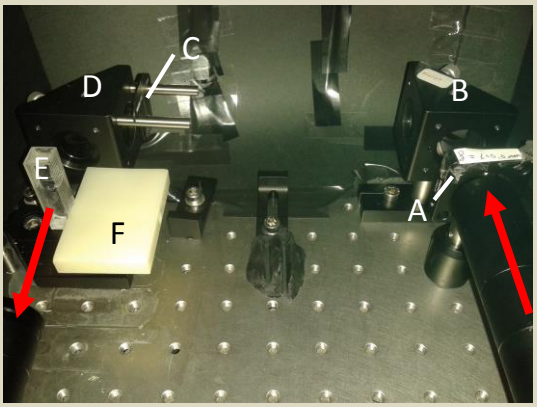

Figure 21

Set up for obtaining images

A) 100mm lens
B) Mirror
C) Alignment target
D) Mirror
E) Cuvette; place to put the other scattering samples.
F) Scattering piece of plastic
The arrows show the direction of the light, from the laser (right) to the camera (left)

To try to solve for this, different combinations of milk (more than 20) were tested until the light pulse were no longer visible; this happens when 600 μL of full milk are dissolved in 3 000 μL of water.

The main problem found was the as more milk added, SNR decreased more rapidly than the amount that it is stretched. In fact, the best images were obtained at very low milk concentrations.

To try to find for a solution, a super-resolution technique was implemented. This consisted on scanning the pulse with a much shorter increase in the delay to take an acquisition in the next pulse, compared to the integration time. This produces

an overlap in time, which is used to sum (in a Matlab program) all the overlapping data and to divide by the number of binned samples. *Figure 22* represents a representative example of an intensity profile.

Other way to try to find a solution was to use the Integrate On Chip (IOC) mode, which is a mode of the camera which allows it to accumulate many acquisitions on the CCD chip, producing one single acquisition with lower noise as if the images would have been summed by software. This is because the readout noise is only added once, since the image is only read once they are already summed on the CCD chip.

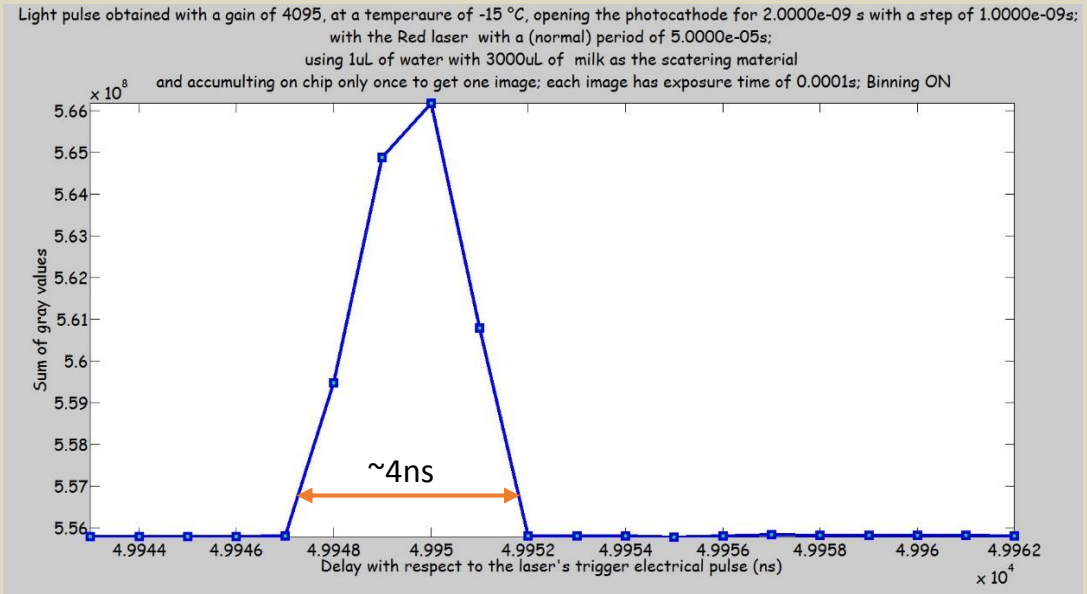

Figure 22

Intensity profile using super-resolution

As can be seen, this combination of milk and water can stretch the pulses from less than 100ps to ~4ns. The optimal gating time would be 49 949ns delay from the trigger pulse.

Notice that the information that is shown in the title was systematically stored in the name of the .tiff file were the image series was stored. 'Binning ON' indicates that the super-resolution technique has been used

Each point represents the sum of grey values of every image obtained at a different time

The width which is shown, corresponds to the full width at 10% of the maximum

The distance travelled through the scattering sample was 0.50±0.05cm

In this case, this mode was used in an attempt to increase the signal in the CCD chip so that the camera can obtain some signal for times shorter than the minimum gating time; unfortunately, this idea did not work, even if all the possible light pulses (period of 50μs) that arrive in 7s were summed. The main problem was that when the pulse was reconstructed a straight line was obtained.

Notice that the camera explicitly asks the operator not to the IOC mode if the external trigger source is faster than 15 kHz. However the minimum selectable

trigger frequency of the laser was 20 kHz. This was just a test to make sure that all options were considered.

Similarly, the Full Vertical Binning (FVB) mode, that is, to sum on chip the recorded data to have only one line, instead of obtaining images was tried, but it did not help to find the optimal gating time as it made it more difficult to visually see the light pulse when looking at the one-line 'image'. In addition, even if the data obtained using this mode was very fast to be processed (as there were less points) to obtain the intensity profile, the results were not better than those obtained with milk dilutions. Finally, it was more challenging to apply the analysis techniques explained in the next section to quantify the improvements in resolution.

Finally, dilutions with paint, cheese and their combinations were also tested, with negative results, since they also suffered from the aforementioned problem: the signal was too weak for high scattering samples, but if the scattering was too low, then only one or two points were obtained in the intensity profile (like in the experiments with milk), which was not enough to find the optimum time delay with enough confidence on the data.

3.4 Analysing the recorded images

Once the pulse was stretched in time, and the optimal gating time was bounded, the next to follow was to find a quantitate way to see if the scattering in the image was reduced. Two ways were proposed:

1) Approximating the PSF. The PSF is the response of an imaging system to a point source, and it is way qualitative way to known the aberrations and resolution of it. The PSF can be approximated by the derivative of a profile around an edge, notice, however, that strictly speaking this should be called Edge Spread Function (ESF). Once it is obtained, it is approximated by a Gaussian function, in order to obtain the Full Width at Half Maxima (FWHM), and thus to have a good estimate of the resolution. Unfortunately, the images had such a low SNR that the matrix that was used to solve a linear system when fitting the ESF to a Gaussian was singular, and the results were unreliable.

2) Measuring the width of the light passing through the pinhole. Unfortunately, the decrease in the laser pulse width due to the possible reduction of scattering was insignificant, ~1-3 pixels in the best scenario.

3.5 Final decision

Even if the light pulse was able to be stretched in time to a measurable extend thanks to the use to super-resolution techniques, it was impossible to be sure

that that the resolution of a biological sample in a scattering media would significantly improve if the SPIM set-up was implemented using this idea. Hence, other synchronization method was considered instead of further developing the 'imaging at the next pulse idea'. In addition, the red laser was left behind due to its low power, and other methods were explored.

4. IMPLEMENTATION OF 'DELAYING THE LASER'S LIGHT PULSES'

4.1 Assessing feasibility

When implementing this idea, the first question that must be answered is *how much* should the light pulse from the laser be delayed so that the camera can image the light pulse after it receives the electrical trigger from the laser?

To give an answer to this question, an oscilloscope was used to measure the elapsed time from the trigger pulse to the opening of the photocathode, i.e. the first peak of the gate pulse, *Figure 23* .

From this, it was found that the *overall* (including wiring, time to reach a threshold level, time to open the photocathode, etc.) minimum achievable delay in the normal, normal with intelligate and ultra-fast modes of the ICCD camera are 161±4ns, 160±4ns and 59.6±2ns for the green laser and 163±10ns, 161.0±0.4ns and 60±0.2ns for the red one.

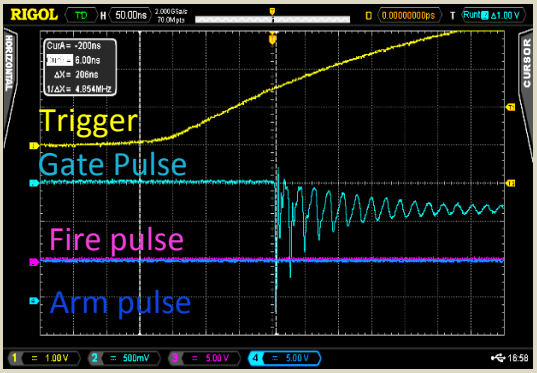

Figure 23

Measurement to obtain the delay of the green laser in the normal mode

Channel 1: Trigger pulse coming from the green laser. Note that the time scale is zoomed so that only the raising edge of the thin pulse is seen

Channel 2: Gate pulse

Channel 3: Fire pulse

Channel 4: Arm pulse

As can be seen, for measuring the times, the author started measuring it from the very first instance the trigger pulse starts going up

With regard the time errors, they were calculated only looking at the time resolution that was available when using the oscilloscope. In other words, the possible error that can happen when selecting the right points on the screen to measure the distance between them, is assumed to be 0, since it is very difficult to quantify it and in most cases it is negligible.

For instance, one way that could have been applied to estimate such an error would have been to select the points three times and take the standard deviation of them.

Briefly stated, in the normal mode ~100ns of time delay are added to the opening of the photocathode. This is because if the intelligate option is also selected, the MCP will be gated as well, thereby increasing the opening/closing efficiency of the camera. In the ultra-fast mode only the photocathode is gated as fast as possible.

Notice that those times are already the minimum achievable ones by reducing the threshold voltage in the camera to start taking the acquisitions. The threshold was set to 0.30±0.01V, which is the minimum allowed value that can be set by software. Due to the fact that the noise in the wires was ~0.1V, the threshold was three times higher than the noise level, so this low value did not compromise the results.

It was also checked whether the delay times could be reduced by changing the terminal impedance of the camera, in case it uses two different circuits, and that one of them is faster than the other. However, if the impedance is set to low (i.e. 50Ω) then the low impedance circuit of the camera takes most of the current thereby dropping the voltage value so that the camera does not reach the aforementioned threshold value. Hence, the impedance that was used for the previous measurements and for the other acquisitions was high (1MΩ).

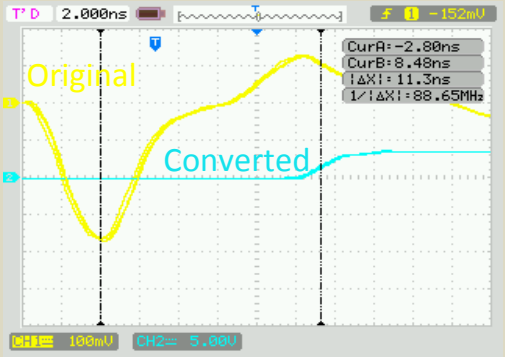

Figure 24

Time response of the TTL converter in isolation (using the minimum needed wires)

Channel 1: Original NIM signal from the red laser

Channel 2: Converted signal to TTL

As before, the trigger signal is just a short pulse,

Notice that the delay is not the same for the two lasers. This happens because the red one produces a NIM standard signal for the trigger pulse which must be converted to the TTL standard signal that the camera expects. Hence, a TTL converter was used. Not only does the converter add more wiring to the system, but also it takes 11.30±0.08ns to react and convert the NIM trigger to 2.5 V in the TTL, *Figure 24*. The TTL converter needs a continuous 5V voltage source; for that, the travel charger ETA0U10EBE, was cut to able to connect the back wire (ground) and the white one (5V) to the converter. Before connecting it, the ripple voltage

was measured to be ~70mV. This value was proved to be more than enough for the correct functioning of the converter.

4.2 Final decision

Therefore, taking into account that the speed of light in air is around $\frac{30cm}{ns}$ [21], (inside the fibre light should travel slower, but this is just an upper bound) the minimum reasonable fibre length would be 18m for the smaller possible measured delay.

But worse than that, other measurements revealed that the **light pulse is sent before the electrical trigger of the two lasers**. Hence, the needed length to delay the light is **greater than 18m**.

18m was already a distance unfeasible get by neither mirrors (as it would be very difficult to align them, and there was not enough space nor large amount of mirrors available), optical fibres (the estimated price is higher than €500, which was not a feasible option for this project) nor separating the camera and the laser (then, other people would not be able to work simultaneously in the lab).

Other drawback is that when the pulses travel that relatively long distance, they will stretched in time a certain amount (especially if an optical fibre is used). Fortunately, such an amount would have been almost negligible [22].

This is why this idea was not furthered developed. And other methods were considered.

5. IMPLEMENTATION OF 'TAKING IMAGES AT A FIXED RATE'

5.1 Green laser: From unpredictable to 2.6ns accuracy

In order for this idea to work in practice, the laser light pulse must be confined to some time-window, otherwise, the needed time to scan the pulse with a reasonable time resolution would be of the order of hours, as the reader could understand when this idea was presented.

Waiting several hours might even be reasonable to draw the needed intensity profile to know the optimal gating time. However, if this idea is to be implemented in a SPIM or any imaging system, then waiting for hours to get one single projection will not be feasible, as the sample itself may be damaged from being exposed to a laser for so long. This is especially important in fluorescence microscopy (i.e. a type of emission microscopy where an excitation light makes some particles called fluorophores to emit light) is performed, since fluorophores are prone to be photo-bleached.

To do it, the green laser, i.e. the only one for which it makes sense to apply this technique, was analysed in detail. It was found that it does not produce any light pulse unless a 5V 'enable' signal is connected to the interlock circuit of the laser. So, the wire was cut and a connection to one of the controllable external outputs of the camera was made, in order to see if the laser pulses could be confined to a small time window when the output of the camera makes the 'enable' signal have 5V. *Figure 25* confirmed this hypothesis.

It was found that if the **output A is allowed to stay high for 0.25ms**, then one single pulse which is **confined to 50ns** is always produced.

Once the pulse was constrained in time, the trigger pulse was recorded *at the same time* that the acquisitions were taken with the camera, in order to know *when* the camera took the acquisitions so that they can be sorted afterwards.

Needless to say, for this idea to work, the oscilloscope and the camera must be synchronized. To do it, the LabVIEW program used for recording the trigger pulse was modified so that it retrieves all the data points which are currently displayed on the oscilloscope screen every 50ms, then it will **store the data in the binary file only if it is different (at least in one point) from the previous ones**.

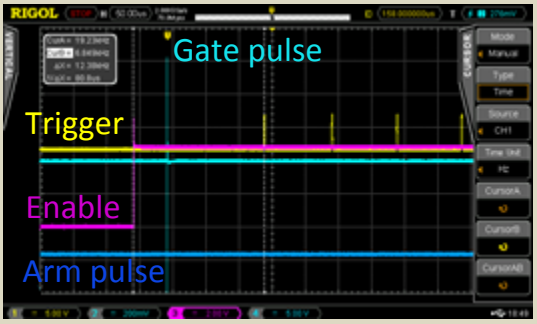

Figure 25

Reducing the laser's uncertainty

Channel 1 (Trig): Trigger from the laser, indicating that it only produces light if the 'enable' signal connected to the camera is HIGH (5V)
Channel 2 (Gate): Gate pulse
Channel 3 (Enable): Output A of the camera connected to the interlock circuit
Channel 4 (Arm): Arm pulse

Then, the following steps were followed: 1) The oscilloscope is set in the 'normal' trigger mode, i.e. it will update the data on the screen each time that the trigger voltage is reached 2) The trigger voltage is set to be the half of the negative peak of the gate pulse, that is, the moment the camera is allowing light to reach the photocathode 3) Using the 'video mode'(that is, to continuously take acquisitions with the camera) the gate delay is adjusted so that the camera is taking pictures more or less when the light pulse arrives. In addition, the position of the gate pulse on the screen is written down. Then the video mode is stopped 4) The LabVIEW program starts recording the data 5) The camera is programmed to take a series of acquisitions in succession, with a frame rate greater than 0.3s by means of the 'Kinetic mode'.

As the probability that the 700 values on the oscilloscope's screen with a 16-bit resolution are exactly the same for two different screenshots is clearly negligible

(and in fact, this did not happen in the more than 40 experiments performed), after following the aforementioned steps, the position of the trigger pulse with respect to the instance when the image was taken is obtained for every picture.

However, shortening in time the samples was not enough to reconstruct the intensity profile, **as the laser sends light pulses with significant pulse-width differences**. Fortunately, **an empirical relationship** (the exact mechanism is unknown) was found between the pulse-width of the light and that of the electrical trigger pulses.

For example, in the Complementary movie 2, the reader can see the pulse reconstruction if the samples are only sorted in time, and in Complementary movie 3, the samples are first selected using a narrow threshold for their electrical pulse-widths, and then sorted to make the second reconstruction.

The 'half-moon' shape that is seen was produced by placing one rounded end of the alignment tool, which was partially covering the laser in front (not at the back) of the scattering sample. The red 'x' represents the reference point (computed as previously described when computing the time error of the trigger pulses) used to sort the samples with respect to the black line, which represents the point in which the camera was taking the image. Notice that the colour-mat is optimized for *every* image, so that the pulses can be seen, at the expense that the series of images seems to 'flash'. A fixed colour-map was rejected as it made it very difficult to see the pulses. Finally, notice that some overlap is present, that is, more than one image was integrated at the same time and they have similar, but not equal values due to the noise in the images.

This is done by means of a Matlab program (downloadable from the annex) which is written as a user interface, since the optimal threshold values changes from acquisition to acquisition, *Figure 26*.

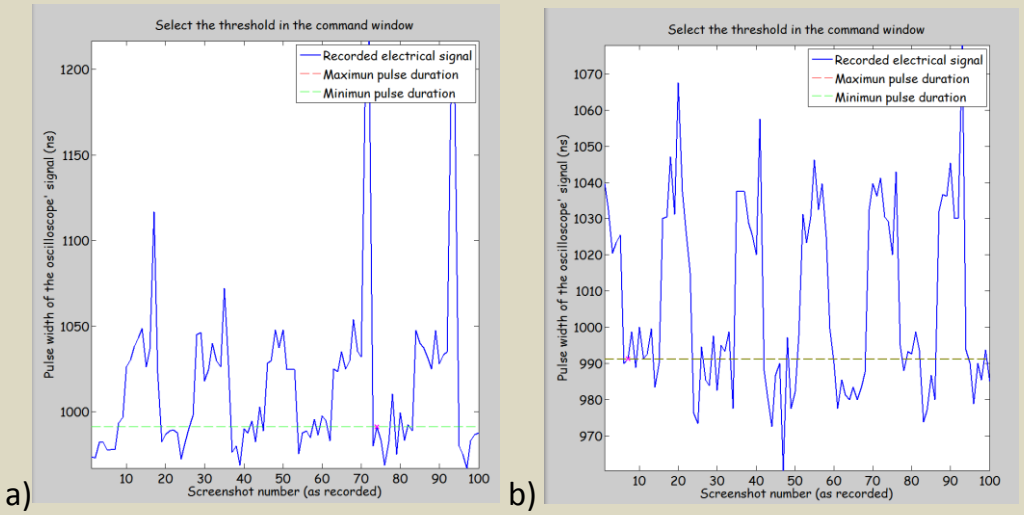

Figure 26

Stochastic behaviour of the trigger pulse width of the laser in two different acquisitions

a) Pulse-width of the electrical trigger for each of the 100 acquisitions in a series

b) Pulse-width of the electrical trigger for each of the 100 acquisitions for a different series made ~5min after the first one

In conclusion, if many pulses sent by the green laser are selected by their pulse-width, and then sorted in time with respect to gate pulse, the acquisitions can be sorted with a 2.6ns accuracy, which correspond to the minimum time scale of the oscilloscope at which is the whole pulse fits on the screen and thus the pulse-width can be calculated from it.

Notice that ~40 points are usually selected from 600 acquisitions, after waiting for ~1min. This is reasonable, knowing that a predictable laser with similar characteristics would have cost around four times more. Hence, the program make the laser give more service than it was payed for.

5.2 Obtaining images

Once the green laser was made predictable (at the expense of waiting until it sends an appropriate set of pulses) a series of different experiments were made, where big scattering materials were used to make sure that scattered photons are more delayed, so that the image quality can be improved in a measurable amount.

For example, a 30.00±0.05cm long aquarium was filled with diluted full milk (1milk:10 water in volume) and all the plastic phantoms were placed in succession, *Figure 27* .

Other experiments include using an 8.00±0.05cm plastic box filled with up to 24 combinations of milk and water.

When focussing this camera (as explained before), reflective neutral density filters were used in order to reduce the power of the laser. For this particular laser, a filter with an Optical Density (OD) of at least 3 was needed.

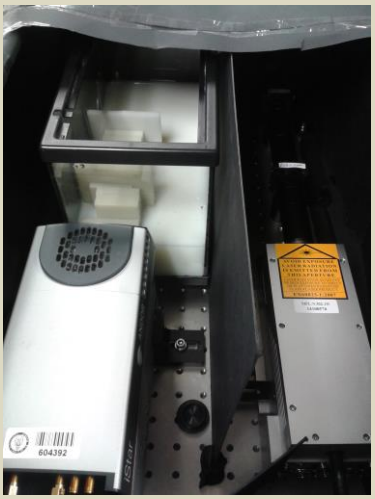

Figure 27

Stretching the light pulses

As in the previous experiments, two mirrors and two lenses were used to widen and cast the laser light on the objective

In this particular set-up, no lens was used due to the lack of space

Note that the name 'neutral' in this context means that all wavelengths are attenuated by more or less the same amount. The term 'reflective' is used because the filters were actually imperfect mirrors, so to say, since they only reflects part the light that is cast to them, allowing the other to pass through them.

The reflective filters were placed so that the beam passes through the lenses before it is reflected by the filters, preventing that the back reflection is not collimated when going into the laser again.

5.3 Analysing the images

With all the different measurements, the idea not only was to find the optimum gating time, but also to find the relationship between the increase in the resolution that the time gated set-up could offer, as a function of the milk content. This would be the first step to know how much better an image could get using the time-gate system as a function of the scattering coefficient.

However, soon, it was discovered that there was a **trade-off which couldn't be satisfied**:

1) If the scattering sample is too scattering, then there are very few photons which are scattered, and thus the increase in the resolution is negligible as the loss in the signal becomes too low. A solution to this, would be to take many more points so that taking the average the SNR can be increased.

2) If the scattering sample has low scattering properties, then it is impossible to discriminate the scattered from the non-scattered photons, due to the fact that

the camera has a minimum gating time of 2ns. As a rough estimate, scattered light must be travelling an extra path length inside the sample of around $\frac{30cm}{ns} \times 2ns = 60cm$ more than non-scattered light, so that scattered and non-scatted photons can be discriminated using the iStar.

Other relationship that was tried to be described empirically and quantitatively, was the time widening of the light pulses as a function of the fraction of milk. It was possible to show that the bigger the proportion of milk is, the bigger the pulse will be in time. However, again, due to the aforementioned problem, the pulse was stretched only one to two gaiting times when high scattering samples were used.

Figure 28 describes the widening (at 10% of the maximum) of the light pulse in time as a function of the sample in the next page.

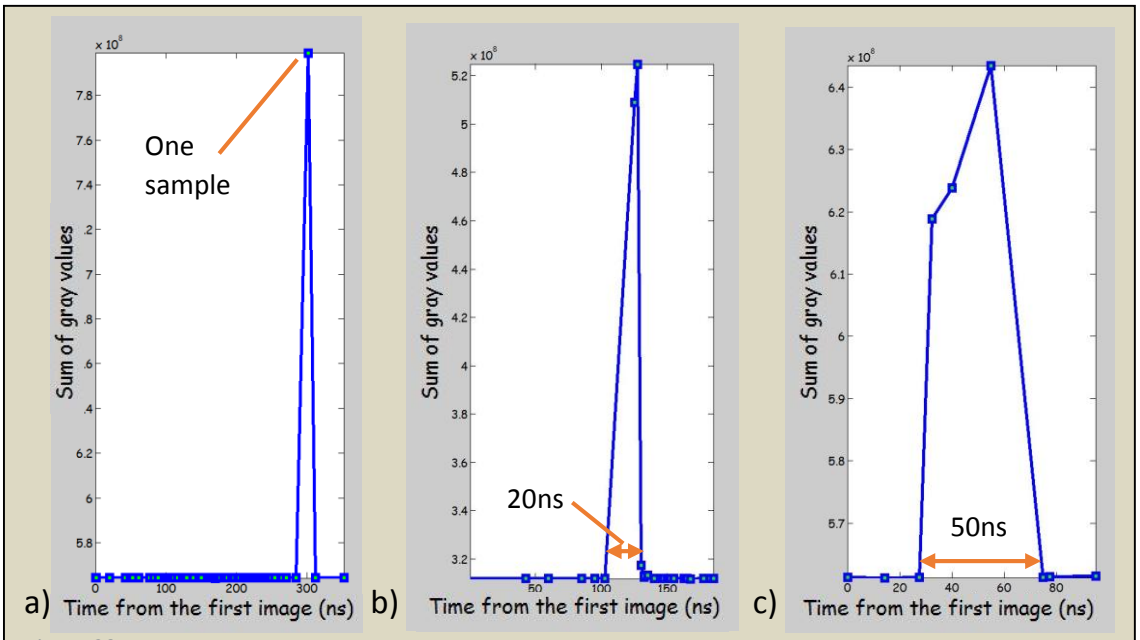

Figure 28

Stretching the light pulse depending on the scattering sample

a) Reconstruction of the pulse without scattering material (only reflective filter with OD=3)

b) Reconstruction of the pulse after passing through 8.00±0.05cm of full milk

c) Reconstruction of the pulse after passing through the scattering material shown in *Figure 27*

5.4 Final decision

Even if the pulses were stretched for around 50 ns, which is way beyond the ~5ns light pulse width of the green laser, this last idea could not significantly improve the resolution of the images (using the aforementioned techniques for the red laser).

As it happened with the previous experiments, there was **a trade-off which could not be satisfied**. The short gate time of the camera requires that the sample has

high scattering properties, so that the scattered photons are delayed by a measurable amount. However, if this first condition is satisfied, then *most* photons arriving to the camera are already scattered (even the first arriving ones), so the improvement was insignificant.

In fact, *reduced* when integrating only the first portion of the light coming out of the sample. This happens because most all the photons that arrived to the detector were scattered, so the effect of reducing signal when integrating only the first portion of the pulse, is much greater than the possible improvement made by looking at the scarce less-scattered photons.

Hence, it was decided not to implement the SPIM, as doing so would not be new from an ordinary SPIM if the negative effects of light scattering could not be significantly reduced.

Block III: Conclusions and outlook

1. CONCLUSIONS

1.1 Scientific conclusions

The main points of this thesis are:

1) A camera with a gating time of 2ns is arguably too long to implement the time-gated set-up for weakly scattering samples.
Then, when the first portion of the pulse is selected, the image quality is reduced as the signal is reduced, without increasing the sharpness as the forward travelling photons cannot be discriminated from those which have been scattered, based on their arrival time.

2) An unpredictable laser can be turned into predictable, provided its electrical trigger pulse is directly related to their light pulses, both in time and pulse-width.

3) A light pulse can be widened in time if an appropriated amount of milk is used. Note that this is one of the very few publications in which large amounts of milk has been used. For comparison, many authors consider a success if they can work with 1.5mm of milk [23].

1.2 Secondary conclusions

1) A camera with an extremely high gain can be safely operated in a room with the lights on, if a stable light proof cage made of cardboard is built and tested.

2) The super-resolution algorithm developed by [20] for registering images can be used to compute the time error of a cyclic process with a resolution greater than the sampling frequency, in a robust and fast way.

3) Binning the overlapping samples when scanning a pulse can be used to go down the minimum gating time of a camera.

4) Approximating the PSF of an imaging system by taking the derivative of a very blurred edge, is not reliable.

5) The iStar is a very optimizable camera, since it has many parameters which can be adjusted for a particular experiment. It can work at very low light illumination levels, -5° of cooling temperature are more than enough to reduce noise. However, it is not suitable to implement the time-gated idea.

1.3 Other kind of conclusions

1) When implementing new ideas or doing research it is very important to regularly interchange ideas with other people, in order to find solutions more efficiently.

2) Technology is very expensive. The low accessibly to high quality equipment may slow down the scientific discoveries.

2. OUTLOOK

2.1 Future work

This thesis has tried to be the first one in improving the quality of biological samples by reducing the scattering. However, this has not been possible, due to the 2ns gate time of the camera used, which made it impossible to develop the so-called time-gated idea.

Hence, the next step will be to acquire a camera which has a must shorter gate time (like those made by LaVision), ideally in the order of the femtoseconds (**using other camera techniques** to make it open and close extremely fast), as it was used in [2]. However, one may also consider cameras in the picosecond range, as they have successfully been used in [1] and [3].

Using the software and methods developed in this thesis it should be straightforward to improve the images in SPIM, for instance.

Once this is done, the next step will be to perform the most important experiment that could not be developed in this thesis, namely: obtaining the improvement in resolution that the **time-gated idea can offer as a function of the scattering properties of the sample**. For this, precise dilutions of titanium dioxide with water will be used to get samples with known scattering properties.

This will be very useful, because such a relationship is still known. Knowing this will allow biomedical engineers know in which applications would this time-gated idea will be worth to be implemented. For example, if the quality of the projections of given scattering tissue is low, one may measure its scattering coefficient, and look in a table if there would be a significant improvement if this idea is put in practice.

Finally, if after finding the relationship one finds a feasible medical application, then, an infrared laser which has a wavelength such as it is less absorbed by the main tissue absorbers (haemoglobin, melanocytes and water) should be used, in such a way that the energy of the pulsed laser can be reduced. Recall, that high energy lasers are needed, as the integration time of the camera must be short. Hence, the best solution would be to decrease absorption rather than to increase the power of the laser.

Block IV: Bibliography

1. REFERENCES

1.1 References used throughout the text

[1] Gordon M. Turner, J. Ripoll and V. Ntziachristos, “Complete-angle projection diffuse optical tomography by use,” *OPTICS LETTERS,* vol. 30, no. 4, 2005.

[2] Michael R. Hee and E. A. Swanson, “Femtosecond transillumination optical coherence tomography,” *OPTICS LETTERS,* vol. 18, no. 12, 1993.

[3] A. Bassi, D. Brida, C. D’Andrea, G. Valentini, R. Cubeddu, S. D. Silvestri and G. Cerullo, “Time-gated optical projection tomography,” *OPTICS LETTERS,* vol. 35, no. 16, 2010.

[4] A. C. Kak and M. Slaney, Principles of Computerized Tomographic Imaging, IEEE Press, 2001.

[5] Basson CT, “Mutations in human TBX5 [corrected] cause limb and cardiac malformation in Holt-Oram syndrome,” *Nat Genet,* 1997.

[6] Pavlos Mihas, "A Historical Approach to the Teaching of the Linear Propagation of Light, Shadows and Pinhole Cameras," *Springer Link,* vol. 14, no. 7-8, pp. 675-697, 2005.

[7] R. Nave, “Blue sky and Rayleigh Scattering,” *Hyperphysics,* 2010.

[8] J. R. Lorenzo, “Light Absorbers, Emitters, and Scatterers: The Origins of Color in Nature,” in *Principles of Diffuse Light Propagation*.

[9] S. L. Jacques, “Optical properties of biological tissues: a review,” *Phys. Med. Biol.*

[10] E. Okada, “Light propagation in tissue and diffuse optical imaging of brain function,” *Biophotonics 2004. APBP 2004. The Second Asian and Pacific Rim Symposium on ,* pp. 125 - 126 , 2004.

[11] N. Menn, “Practical Optics,” *Academic Press.*

[12] ANDOR an Oxford Instrument company, “Intensified Camera Series,” [Online]. Available: http://www.andor.com/scientific-cameras/intensified-camera-series?gclid=CIb40-KMj8YCFQTLtAodIS4AYQ.

[13] Changchun New Industries Optoelectronics Technology Co., Ltd., “MPL-N-532/40~125uJ/150-1000mW - up to 125uJ, 532nm passively Q-switched pulsed green laser,” [Online]. Available: http://www.cnilaser.com/MPL-N-532.htm.

[14] Edinburgh Instruments (Phtonics Division), “The EPL Series: Picosecond Pulsed Diode Lasers,” 2014.

[15] Andor Technology, “New iStar ICCD (User’s Guide),” 2012.

[16] J. Maljaars, J. Fellinger and F. Soetens, “Fire exposed aluminium structures,” Eindhoven, the Netherlands.

[17] Scientific Volume Imaging, “Airy disk,” [Online]. Available: https://svi.nl/AiryDisk.

[18] Smith, “Risk perception and communication: recent developments and implications for anaesthesia,” *Anaesthesia,* pp. 745-755, 2001.

[19] Marmad; Teneyes, “Software & tips for Rigol DS2072 (DS2000 / DS4000 / DS6000 UltraVision DSOs),” eevblog, [Online]. Available: http://www.eevblog.com/forum/projects/software-tips-and-tricks-for-rigol-ds200040006000-ultravision-dsos/125/?wap2.

[20] Manuel Guizar-Sicairos, “Efficient subpixel image registration algorithms,” *Opt. Lett,* no. 33, pp. 156-158, 2008.

[21] B. Brody, The Speed of Light: Making an Easy Time of It, vol. 41, Phys. Teach., 2003, p. 276.

[22] A. Karaka and S. Sarkara, “Prediction of modal dispersion in nonlinear single mode optical fiberusing simple Chebyshev technique,” *ELSEVIER,* 2015.

[23] Freudig, L. Tian, P. Polfer and D. C. Zimmermann, “Light Transmission in whole milk: A new method of determining adsorption properties”.

[24] RIGOL Technologies, Inc., "DS1000B Series Digital Oscilloscopes DS1074B,DS1104B,DS1204B," UGA04123-1210 ed., 2014, pp. 2-53.

[25] J. Sharpe, “Optical projection tomography,” *Annual review of biomedical engineering,* vol. 6, no. 1, pp. 209 - 228, 2004.

1.2 Further reading

N. Tsu-Wei, F. N. Soe-Mie, Y. De-Ming and H. Yu-Shan, Scattering polarization by anisotropic biomolecules, vol. 25, Journal of the Optical Society of America A: Optics and Image Science, and Vision.

J. W. G. Hunt, Measuring Color. Ellis Horwood Ltd, 1980.

2. REMARKS

2.1 Disclaimer

All the provided external links in this document are given for academic proposes. The author is not responsible of neither their functionality nor content.

All unsourced materials have been obtained from the author's work. The only exceptions are these images:  and  which were taken from GetSpottedOnline.co.uk and pixabay.com, respectively.

If the reader have problems downloading the code and/or the data, or watching the complementary movies, please contact 100292976@alumnos.uc3m.es

Block V: Annexes

1. DATA PROCESSIONG

1.1 Link to download all the computer software used

Download Software

1.2 Link to download some representative data

Download Data

2. LIST OF MATERIALS USED

2.1 Hardware

Concept (~price [€] including VAT)	Model	Manufacturer	Relevant characteristics/ Comments
2 Aluminium mirrors (90)	PF07-03-G01	ThorLabs	**Diameter**: 19.0±0.1mm **Thickness**: 6.0 ±0.2 mm
2 Fixed Optical Mounts (40)	CP06	ThorLabs	**It can be attached to the table** via a post
2 Mirror mounts (70)	KM05/M	ThorLabs	**Resolution:** 13 mrad (0.75°) per turn via two precision adjusters
3 Lenses (two types) (320)	AC254-060-A-ML AC254-050-A-ML AC254-100-A-ML	ThorLabs	**Include a holder** to screw them to the optical mounts
3 SMA **to** SMA **cables** (120)	CA2736	ThorLabs	**Impedance**: 50Ω **Frequency Range:** DC - 12.4 GHz One of them was adapted to be used in the green laser

4 SMA to BNC cables (160)	CA2612	ThorLabs	**Impedance**: 50Ω **Frequency Range:** DC - 12.4 GHz
Adaptor (30)	SM1A15	ThorLabs	It allows the **camera to be connected to the tubes**
Alignment target (12)	CPA1	ThorLabs	It produces **high contrast patterns**
Attaching elements to the table (posts, post holders…) (300)	TR20/M BA1S BA2 MSCL3 PH30/M RA90 TR6 PH6	ThorLabs	The needed **screws are not included**
Blackout Fabric (50)	BK5	ThorLabs	It is flexible The manufacturer recommends to use **two layers** for extremely sensitive applications
Cage System Construction Rods (70)	SR05	ThorLabs	Use to **hold the alignment target** **Length**: 12.7 mm **Material** :stainless steel
Cardboard (3)	*None*	*None*	It is **black** to absorb as much light as possible
Computer (350)	P6-2112es (HP pavilion)	Hewlett-Packard Company	**Microprocessor:** Intel(R) Core (TM) i3-2120 @3.30GHz **Operating system**: Windows 7 Home Premium (64 bit) **RAM**: 6 GB
Digital Oscilloscope (2 000)	DS4014 (Ultra Vision)	Rigol	**Number of channels**: 4 **Maximum sampling frequency:** 100MHz, 4GSamples/s
Digital Oscilloscope (800)	DS1104B (LXI)	Rigol	**Number of channels**: 4 **Maximum sampling frequency:** 100MHz, 2GSamples/s

Digital Oscilloscope (300)	DS1102E	Rigol	**Number of channels**: 2 **Maximum sampling frequency:** 100MHz, 1GSamples/s
High intensity pulsed laser (15 000)	MPL-N-532 (PSU-H-FDA)	Opto Engine LLC	**Wavelength:** 532±1 nm **Pulse duration**: ~5ns **Safety**: Class 4 **Repetition rate**: Unpredictable from 5 to 15kHz
ICCD **Camera** (30 000)	DH334T-18U-03 (iStar)	Andor	**Max resolution:** 1024x1024 pixels **Minimum gate time**:~2ns It includes many cables, like USB
Lends Tubes And iris(three types) (200)	SM30L05 SM30L10 SM30L30 SM1D12SS	ThorLabs	**Stackable Design**
Micropipette and tips (90)	P3940- 2 P3940-1000 TIPP-1K0-1K0	Labnet Labbox	They were used to make different **combinations of milk and water for the cuvette**
Mobile phone (240)	GT-I8190 (Galaxy SIII mini)	Samsung	**Microprocessor:** 1GHz **Camera**: 5MPixels **Battery**: 1500mAh
Needleless Syringe (10)	TC1504123	Liquid Control Equipment Vic Store	It was used to mixt water and **milk in known proportions for the big plastic box**
Phantoms (30)	*None Handmade*	*None Handmade*	They were used as a **scattering material**
Picosecond pulsed diode laser (6 000)	EPL-670	Edinburgh Instruments	**Wavelength**: ~672.8nm **Pulse width**:~ 67.8 ps **Safety**: Class 3R
Plastic Holders (2)	MAPS-F10-100 *Reused material*	Labbox *Reused material*	The cuvette and plastic box were used to **hold the scattering samples in place** The big plastic box was a **reused packing box** for micropipette tips

Reflective Filters (200)	ND10A ND30A ND40A	ThorLabs	Used to **focus the camera when using the green laser**
Safety Glasses (150)	LG3	ThorLabs	**48% visible light Transmission** Universal Style (they can be worn with prescription glasses)
Scattering liquids (6)	*None* *None*	Carrefour Crown	The **full milk** has 3.6g of fat per 100mL Only traces of **white paint** were used
Screen monitor (including needed wires) (200)	237EQPH	Philips	**Resolution**: 1920 x 1080 pixels Size: 23 inches
Screw and washer kit (90)	HW-KIT5	ThorLabs	It includes all the different screw types needed
Table with holes and supports (8 000)	T1525D PTL702	ThorLabs	**Height Adjustment**: +15 mm/-8 mm **Passive isolation**
Travel charger (10)	ETA0U10EBE	Samsung	**Input**: 100-240V~ **Frequency**: 50-60Hz, 0.15A **Output**: 5V,0.7A
TTL converter (150)	*None Handmade*	*None Handmade*	**Fast conversion time:** <12ns to produce 2.5V in the converted signal
USB **flash drive** (7)	DataTraveler (G3)	Kingston	**Memory**: 8GB **Format**: FAT32

2.2 Software

Concept (~price [€] including VAT)	**Version**
ImageJ (0)	1.6.0_20 (64-bit)
LabVIEW (3 000)	12.0f3 (64-bit)

Matlab Basic and Image Processing Toolbox (3 000)	R2012a(7.14.0739) 64-bit(win64)
Microsoft Office Profesional Plus 2013 (540)	15.0.4727.1000 (32-bit)
Windows Movie Maker (0)	15.4.3538.0513

2.3 Budget

Concept	~Price [€] including VAT
Physical materials	65 100
Software	6 540
Man hours (including facilities, water, electricity, etc.) (310h student @25€/hour) (38h senior @35 €/hour)	9 080
TOTAL	**80 720**

3. *GLOSSARY*

3.1 Abbreviations used in this text

BNC: Bayonet Neil Concelman (connector); refer to this webpage

CCD: Charge-Couple Device

CW: Continuous Wave

DDG: Digital Delay Generator

ESF: Edge Spread Function

FAT: File allocation Table; refer to this webpage

FFT: Fast Fourier Transform

FVB: Full Vertical Binning

FWHM: Full Width at Half Maxima

GFP: Green Fluorescent Protein

ICCD: Intensified Charge Couple Device

IOC: Integrate On Chip

LED: Light Emitting Diode

NA: Numerical Aperture

MCP: Micro Channel Plate

NIM: Nuclear Instrumentation Module; refer to this webpage

OD: Optical density

OPT: Optical Projection Tomography

PSF: Point Spread Function

RAM: Random Access Memory /ræm/

SMA: SubMiniature version A (connector); refer to this webpage

SNR: Signal to Noise Ratio; $\frac{signal}{noise}$ where $signal$ represents the sum of the recorded light intensities produced by a desired signal. Hence, $noise$, is defined in this document as the sum of all other recorded intensities, not being produced by the desired signal. Noise includes photon noise, camera noise, etc.

SPIM: Selective Plane Illumination Microscopy

TTL: Transistor-Transistor Logic (compatible signal); refer to this webpage

USB: Universal Serial Bus

VAT: Value Added Tax

4. DERIVATION OF KEY EQUATIONS

4.1 Derivation of the Beer-Lambert's law of absorption

Consider a medium that statistically and *proportionally* losses λ photons of a given energy after traveling a distance dx in the medium. Then, the rate of change of the number of the current number of photons, N, will be given by

$\frac{dN}{dx} = -\lambda N$. This is a separable differential equation$\Rightarrow \frac{dN}{N} = -\lambda\, dx$. Integrating$\Rightarrow$ $\int \frac{dN}{N} = \int -\lambda dx$.

Recalling that $(\ln y)' = \frac{1}{y}$ and integrating $\int (\ln y)' dx = \int \frac{1}{y} dx \Longrightarrow \ln y + C = \int \frac{dy}{y}$

Substituting in the previous equation$\Longrightarrow \ln N = -x\lambda - C \Longrightarrow N(x) = e^{-C} e^{-x\lambda}$

Since C is an arbitrary constant, so is $e^{-C} \Rightarrow N(x) = Ke^{-x\lambda}$

Solving for the initial condition $N(0) = N_0 \Rightarrow N(x) = N_0 e^{-x\lambda}$

This was done for a particular frequency of the photons, the value of λ changes depending on the type of photon⇒ $N(x) = N_0 e^{-x\lambda(frequency)}$

In addition, if there are several materials in the path that the photons follow, the value of λ will also change depending on the material

$N(x) = N_0 e^{-x_1\lambda_1(frequency)} e^{-x_2\lambda_2(frequency)} \times \ldots \times e^{-x_n\lambda_n(frequency)}$

Using the property that $e^a e^b = e^{a+b}$

$N(x) = N_0 e^{-\sum_{i=1}^{n} x_i\lambda_i(frequency)}$

In the limit when $x_i \to 0$. Finally, $\boldsymbol{N(x) = N_0 e^{-\int \lambda(frequency)dx}}$

Hence, the inverse of the attenuation coefficient, $\frac{1}{\lambda}$, can be understood as the distance, with the same units as x, that the light photons needs to travel in order to get attenuated by a factor of $\frac{1}{e}$.

Another way to understand the equation is that the probability of a photon to continue with its original trajectory after having travelled a distance x in a medium is given by is $Probability(x) = N_0 e^{-\int \lambda(frequency)dx}$